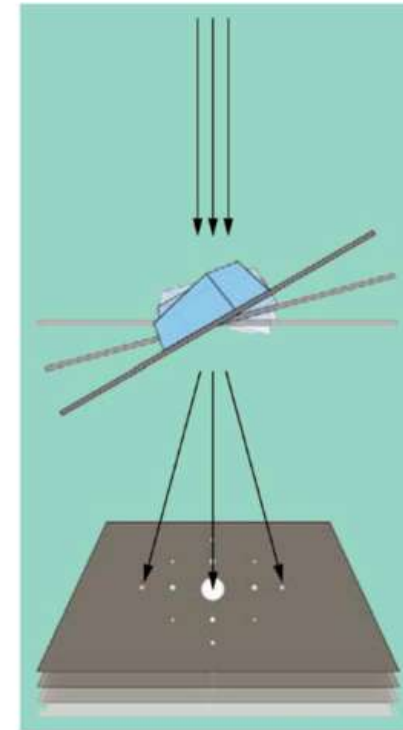
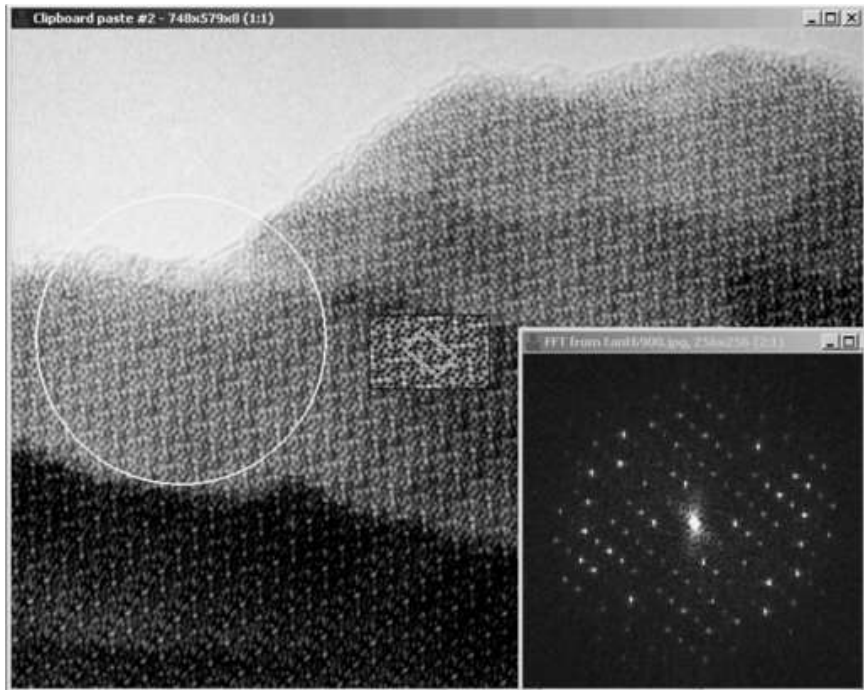
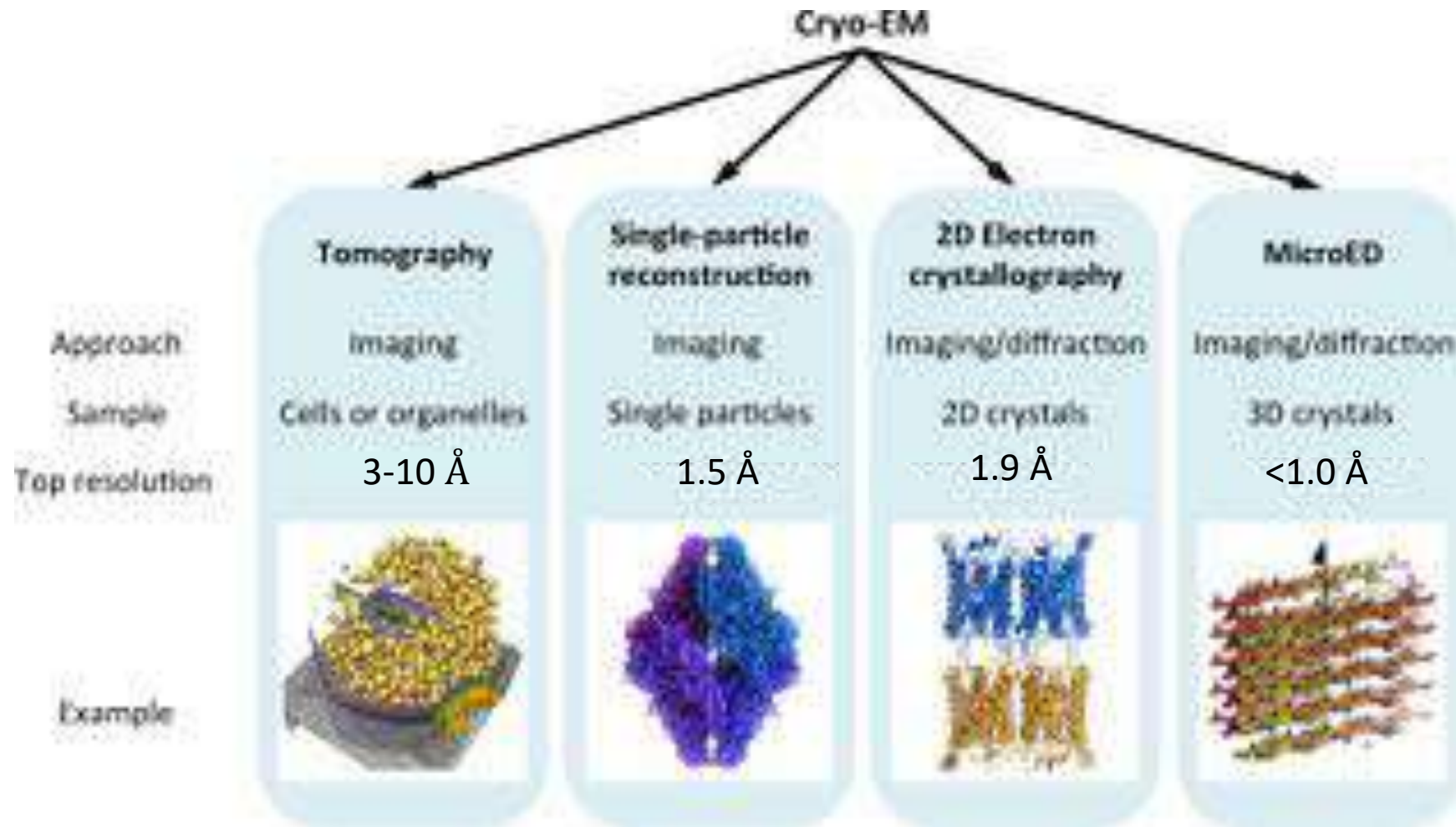


MicroED and 2D Crystallography

Feb. 3, 2020



Best Resolution from EM Techniques

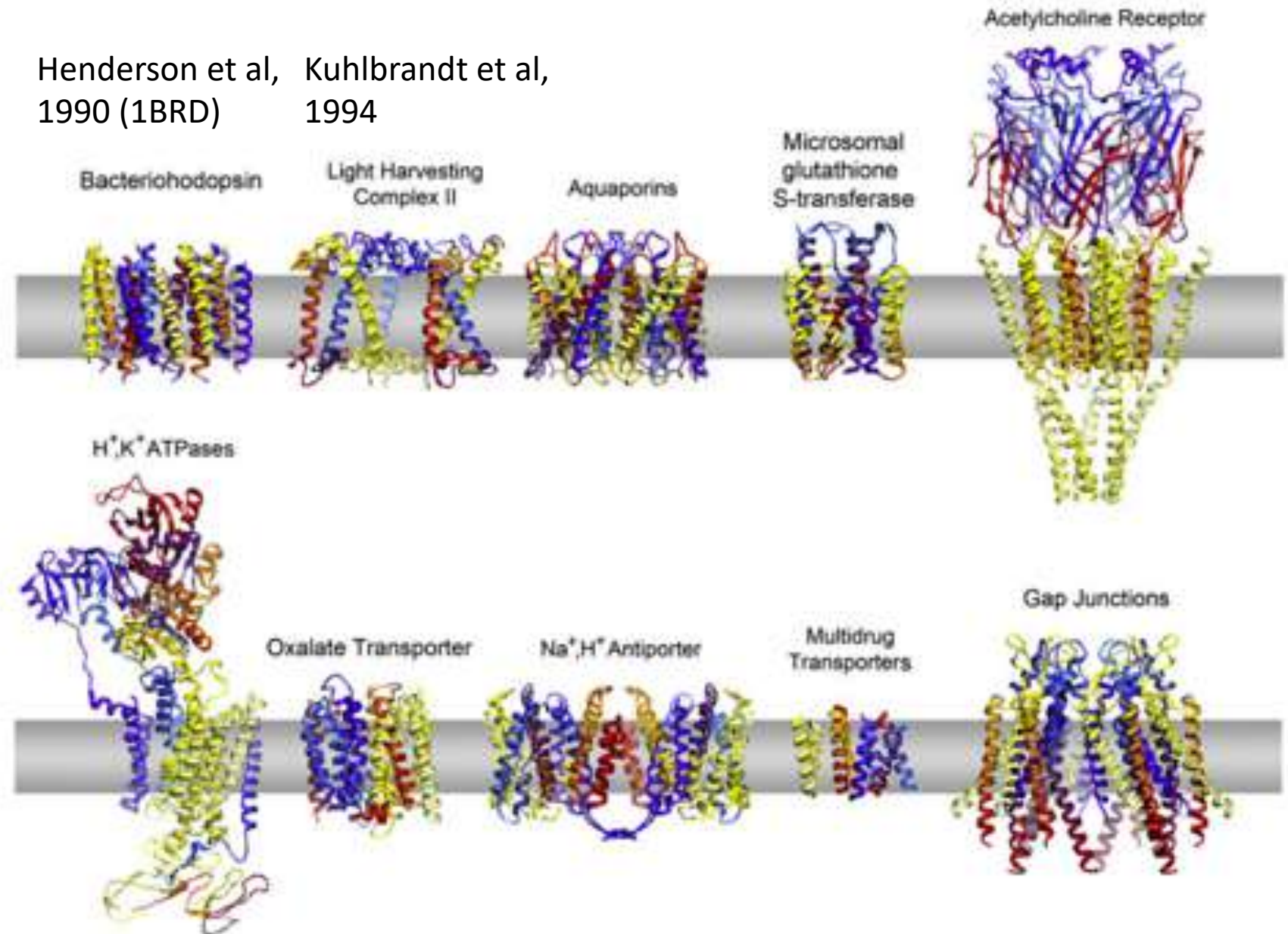


2D Crystallography

The first high resolution Cryo-EM method, mostly for membrane proteins

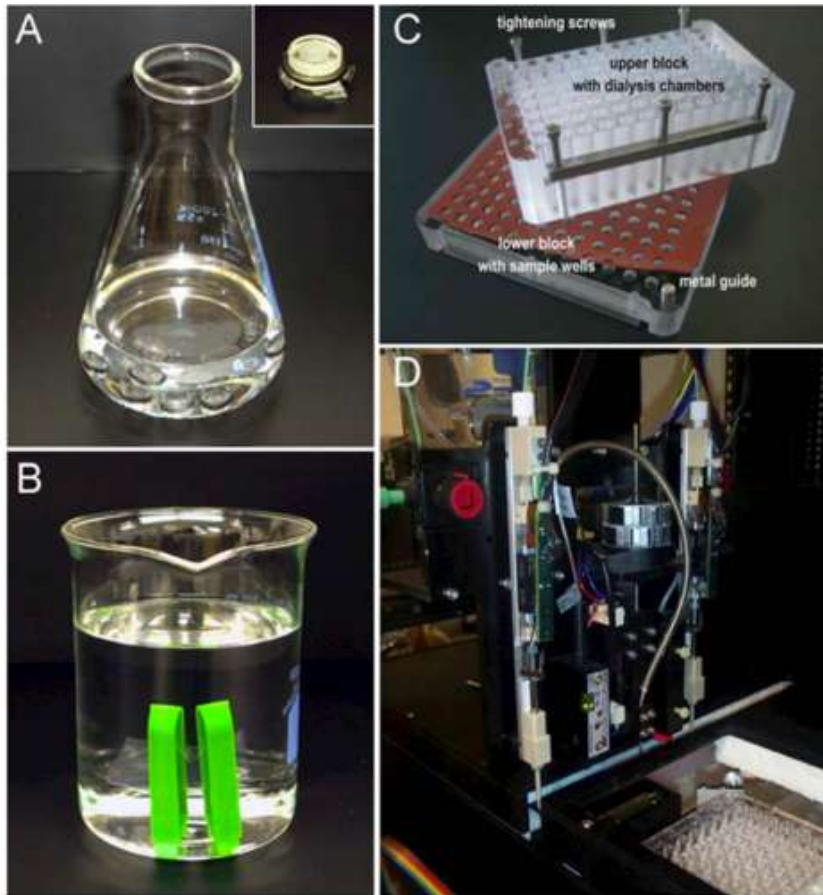
High Resolution Structures from 2D Crystallography

Henderson et al, 1990 (1BRD)
Kuhlbrandt et al, 1994



Wisedchaisri et al, 2011

Preparation of 2D crystals: Remove detergent and put into lipid bilayer



- A: dialysis buttons
- B: Dialysis tubing
- C: 96-well dialysis block
- D: Robot for cyclodextrin mediated detergent removal

2D crystal screening

C

Report Window

- Create Screen Table
- Add Component
- Delete Component
- Add Row to Screen
- Close Row in Screen
- Remove Row from Screen
- Clear Screen Table
- Calculate Volumes
- Change Parameters
- Append Screen
- Add Screen
- Screen Optimization
- Stock Solution Selector
- Refresh Batch No
- Create Droplet Table
- Add Addition
- Delete Addition
- Set Droplet Components
- Clear Droplet Table
- Add Scoring Column
- Remove Last Scoring Column
- Map Screen To Plates
- Clear Plate Table

WE.24 Screen: X28_P2A3

General | Screen Reservoirs | Screen Droplets | Droplet Scores | Screen Plates

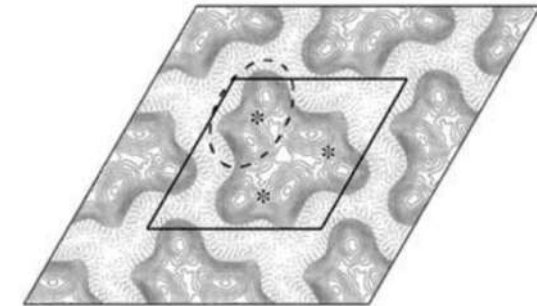
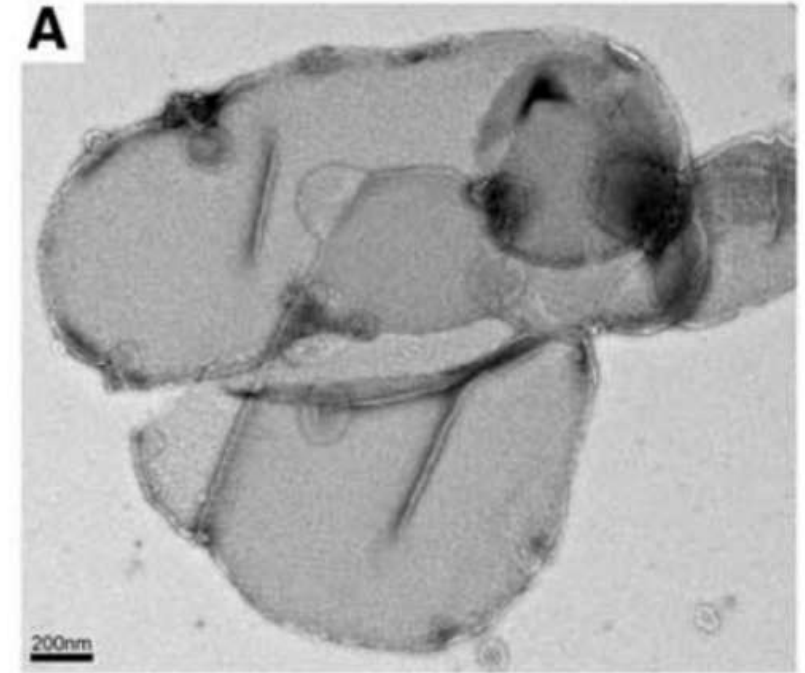
Database No: 24
 Created By: mmk, 2009-12-02 13:18:00.0
 Modified By: mmk, 2009-12-02 13:18:29.0
 Lab: NYDBO 20K
 Labfund:
 External ID:
 Status:
 Type:
 Name: X28_P2A3
 Screen Type: Custom
 User Label:
 Lab Protocol: 508: setting up a 20K screen

WE.43 Screen: X28_P2A3

General | Screen Reservoirs | Screen Droplets | Droplet Scores | Screen Plates

| Well No | pH | Total Vol | H2O Vol (u) | Mix Cyl | Salt List | Conc | Unit | Vol (u) | Batch | Buffer List |
|---------|----|-----------|-------------|---------|-----------------------------|------|------|---------|-------|------------------------------|
| 7 | 0 | 50 | 15.25 | 0 | 480: 1.0 M sodium ascorbat | 25 | mM | 1.25 | 1 | 487: 1.0 M Na-citrate pH 5.5 |
| 8 | 0 | 50 | 11.92 | 0 | 492: 1.0 M sodium citrate p | 25 | mM | 1.25 | 1 | 486: 1.0 M MOPS pH 6.5 |
| 9 | 0 | 50 | 8.58 | 0 | 473: 1.0 M calcium acetate | 25 | mM | 1.25 | 1 | 465: 1.0 M HEPES pH 7.5 |
| 10 | 0 | 50 | 15.25 | 0 | 478: 1.0 M sodium acetate p | 25 | mM | 1.25 | 1 | 468: 1.0 M Tris-Cl pH 8.5 |

Crystal lattice Sheets Proteoliposomes Protein aggregates Lipidic structures Precipitation



Wisedchaisri et al, 2011

Imaging

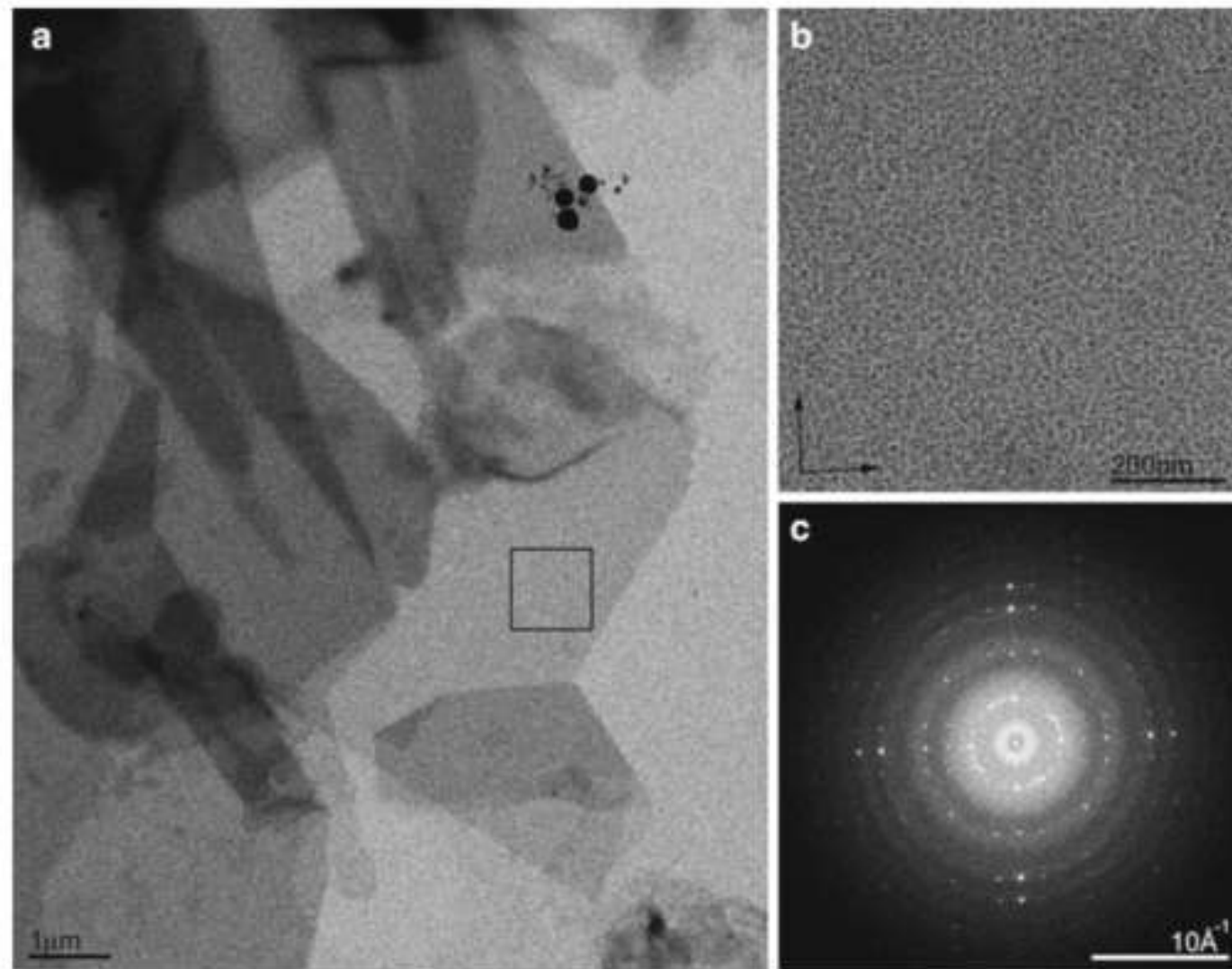


Fig. 3. Cryo EM of two-dimensional crystals. (a) Crystals of the water channel aquaporin-0 are large and have sharp edges attesting to the degree of order within. (b) High-resolution image of the crystal area highlighted by a *box* in (a). (c) Fourier transform of the image in (b) showing strong and sharp spots to $\sim 6\text{\AA}$ resolution. These crystals are ready for analysis by electron diffraction because the crystals appear uniformly *grey* on the grid. The spots in the Fourier transform are sharp and extend to $\sim 6\text{\AA}$ resolution without unbending. At this stage the sample should be frozen and the microscope setup should be changed to diffraction and data collected.

Diffraction data collection of 2D crystals

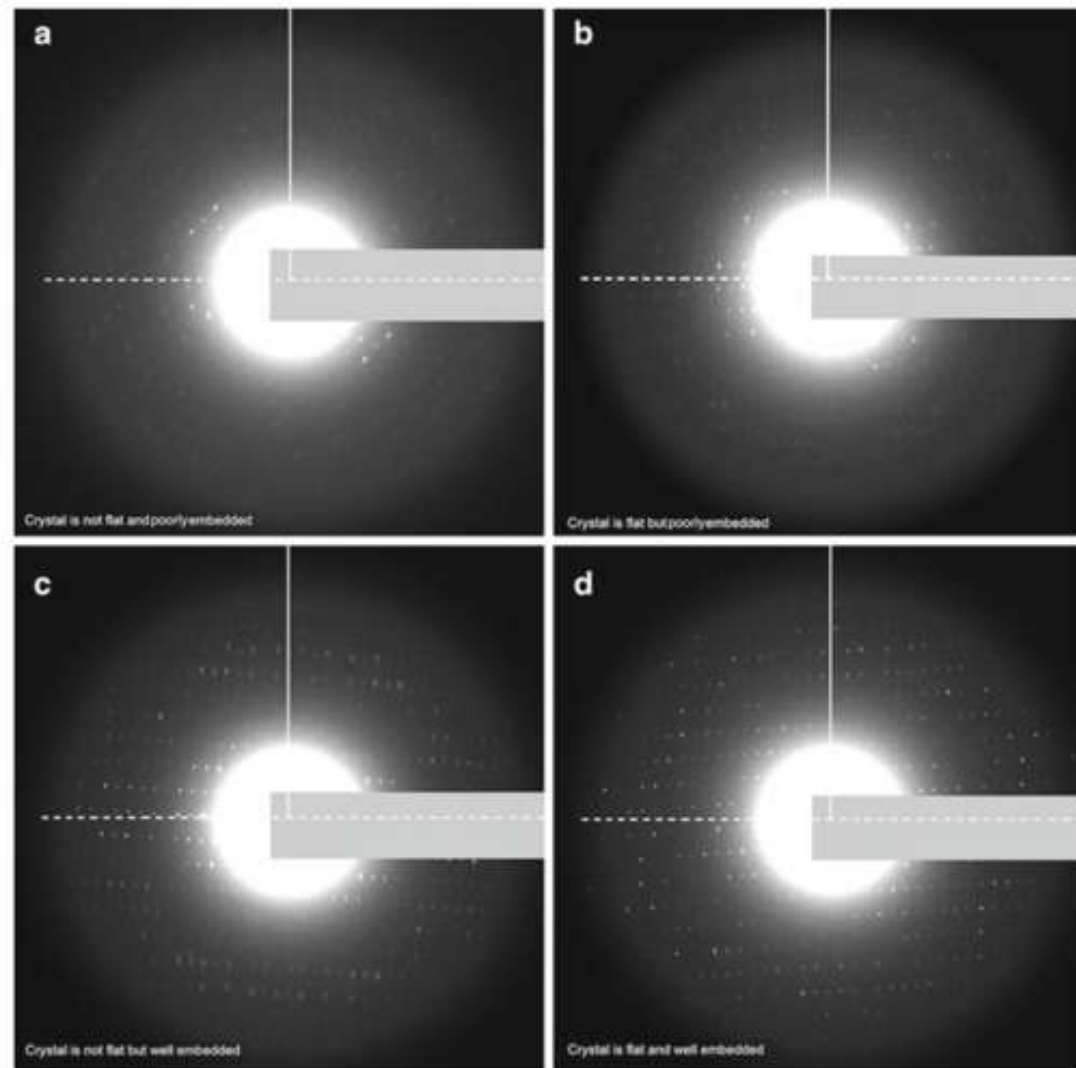


Fig. 4. Assessment of crystal flatness and embedding by electron diffraction. (a–d) The flatness of the crystal will affect the attainable resolution. If crystals are not flat the resolution will be cut off in the direction perpendicular to the tilt axis (tilt axis in *dashed line*, perpendicular to the tilt axis in *solid line*). Likewise, a well-embedded crystal will show strong and sharp spots in the diffraction pattern but a poorly embedded crystal will have limited resolution. (a) An example of a crystal that is not flat and also poorly embedded. No sharp spots are visible perpendicular to the tilt axis, indicating that this crystal is not flat. Only a limited number of spots are visible on the tilt axis, indicating that the crystal is not embedded properly and was damaged during grid preparation. (b) An example of a crystal that is flat but poorly embedded. It is flat because many spots are visible in all directions, even perpendicular to the tilt axis. The crystal, however, is poorly embedded because most of the spots are not sharp and have a weak intensity. (c) An example of a crystal that is not flat but is embedded well. The crystal is well embedded because most spots in the diffraction patterns appear strong. However, the crystal is not flat because only the spots on the tilt axis are sharp, while the spots perpendicular to the tilt axis are smeared. (d) An example of a crystal that is both flat and well embedded. All of the spots in this diffraction pattern are intense and sharp. In all figures the beam stop is masked by the *grey rectangle*.

Setup: 2D diffraction collection (manual low-dose)

Setting up the search mode:

1. Choose the smallest spot size.
2. Set magnification in imaging mode to $\sim 15,000\times$.
3. Turn diffraction on.
4. Change the diffraction length to the largest setting (e.g., 6,000 mm).
5. Focus the beam until you obtain a very sharp spot at the very center of the screen.
6. If the spot is not sharp, use the diffraction astigmaters to sharpen the spot.
7. At the end of this procedure (if done properly) the beam should appear as a triangle with a sharp spot at its very center.
8. Overfocus the beam until an image appears on the screen.

Setting up focus mode (Note 6):

1. In search mode use the wobbler to find the eucentric Z-height.
2. Switch to focus mode.
3. Choose spot size 10.
4. Magnification should be set to $250,000\times$.
5. Set up the distance to $\sim 1.5\text{ }\mu\text{m}$ from the target.
6. Focus the beam crudely at first by using the eucentric focus feature.
7. Focus the beam more finely.
8. Reset focus when the focus is reached (do not defocus at this stage).

Setup: 2D diffraction collection (low-dose)

Setting up exposure mode:

1. Choose spot size 10.
2. Magnification should be set to $\sim 15,000\times$.
3. Spread the beam to ~ 2 cm diameter on the viewing screen.
4. Turn diffraction on.
5. Choose the appropriate diffraction length (see Subheading 3.3.3).
6. Focus the beam until you get a sharp spot at the very center.
7. If the spot is not sharp, use the diffraction astigmaters to sharpen the spot.
8. Insert the beam stopper (Subheading 3.3.2).
9. Use diffraction shift to align the diffraction beam with the beam stopper (Subheading 3.3.2).
10. Insert the CCD and record an image to determine the appropriate exposure time (Subheading 3.3.4).

Data collection in ED:

1. Find a crystal that appears flat and not folded in search mode.
2. Place the chosen crystal area at the center of the screen.
3. Insert the SA aperture and center the SA aperture over the chosen crystal area.
4. Insert the beam stopper (see Subheading 3.3.2).
5. Blank the beam.
6. Switch to exposure mode.
7. Raise the screen and cover the camera chamber with the rubber cover that was supplied with the microscope.
8. Unblank the beam.
9. At this stage the CCD is controlling the shutter, so the crystal is not exposed to radiation damage.
10. Record the diffraction using the appropriate exposure time (Subheading 3.3.4).
11. Once the diffraction is recorded, retract the camera.
12. Lower the screen.
13. Realign the beam behind the beam stopper.
14. Remove the beam stopper.
15. Check the beam for focus and diffraction astigmatism.
16. Remove the SA aperture.
17. Return to search mode.
18. Use the diffraction shift to align the exposed area of the crystal with the center of the screen.
19. Go back to step 1 above and repeat the process for collecting ED data of the next crystal.

Processing: 2dx

A

2dx_Merge

Standard Surges

- Initialization
- First Merge
- Merge & Refine
- Generate Image Maps
- Final Merge
- Generate Merged Map

Custom Surges

- Modify Image Parameter
- Display Maps
- Refresh Databases
- Image Inventory
- Cleanup
- All Parameters

Processing Data - Standard

Lattice Determination

Real Unit Cell Length: 129.129
 Real Cell Angle: 90

Common Image Processing

Upper Resolution Limit: 16
 Lower Resolution Limit: 200

Program Technical Data

Keep Large Temporary Files?: Yes

Symmetry

Symmetry: 94

Merging Data Multifractions

Merged reference exists?: yes, 20
 Resolution of the merged dataset: 16
 Size of the phase origin search: 0.2
 Number of steps in phase origin search: 61

Logfile - Low Memory

```

-----
1.2 10.7 24.9 23.5 12.1 47.4 20.2 10.9
22 35 20 23 12 15 11 38
-----
Overall: Phaseresidual = 30.824 Number of apert = 174
-----
**** average - to transform merge.apf into avg.hal ****
**** 3dx_centroid - to correct phases to 0 or 180 ****
**** 3dxs - to transform HKL file into MTZ file ****
**** 3dxs - to expand MTZ file to cover pi asymmetric unit ****
**** compile refinement script ****
**** Launch refinement script ****
-----
Number Scale Phase Origin Change Phase Ori. Phases
10100333 1.000 166.900,-2.810 0.400,0.000 17.48
1003016 19.095 34.400,156.890 0.000,0.000 22.39
-----
**** 3dx_refine normal end. ****
***** 3dx_refine finished.*****
  
```

Results

Parameter Value

00//ML0010100333

MERGE_TANCL 0.000
 MERGE_TAXA 0.000
 MERGE_TLTANG 0.000
 MERGE_TLTAXA 0.000
 MERGE_TLTAXIS -15.018
 MergePhaseResidual 17.48
 MergeScaleFactor 1.000
 PHASEORI_dome Y
 phaori 166.900,-2.810
 phaoriFouFilter 166.900,-2.810

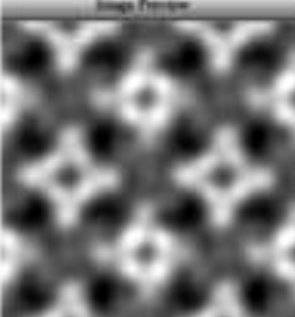
X1-00//ML1003016

MERGE_TANCL 0.000
 MERGE_TAXA 0.000
 MERGE_TLTANG 0.000
 MERGE_TLTAXA 0.000
 MERGE_TLTAXIS -14.322
 MergePhaseResidual 22.39
 MergeScaleFactor 19.095
 PHASEORI_dome Y
 phaori 34.400,156.890
 phaoriFouFilter 34.400,156.890

Images

merge-even/
 APH/merge.apf
 APH/avg.nolimit.apf
 LOC5/phase-residuals.txt
 APH/avg.limit.apf
 HKL/centric.hkl
 SCRATCH/merge-part.mtz
 merge.mtz

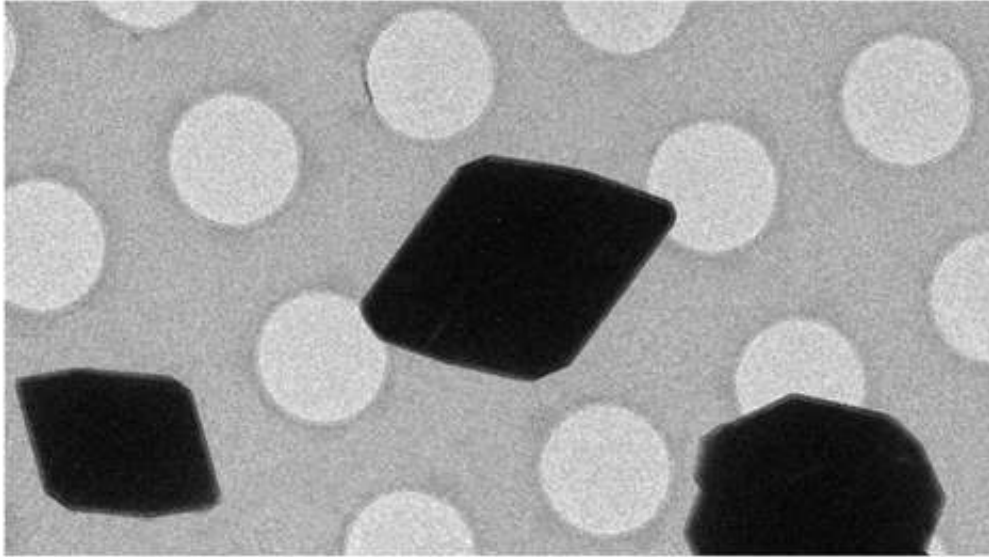
Image Preview



Difficulties in 2D crystallography

- Screening
 - Setting up conditions
 - Screening one by one
 - Large factorial surface (buffer, additives, lipid, detergent, speed of detergent removal)
- Samples
 - Need to be extremely flat over a large area
 - Need to be very well ordered
- Collection
 - Need to merge crystals at different tilts to get 3D reconstructions
 - Collect images as well as diffraction data
 - Hard to collect high quality tilted images
 - Manual collection
- Software
 - Difficult to use: until 2dx, command-line driven scripts

Molecular structures made simple



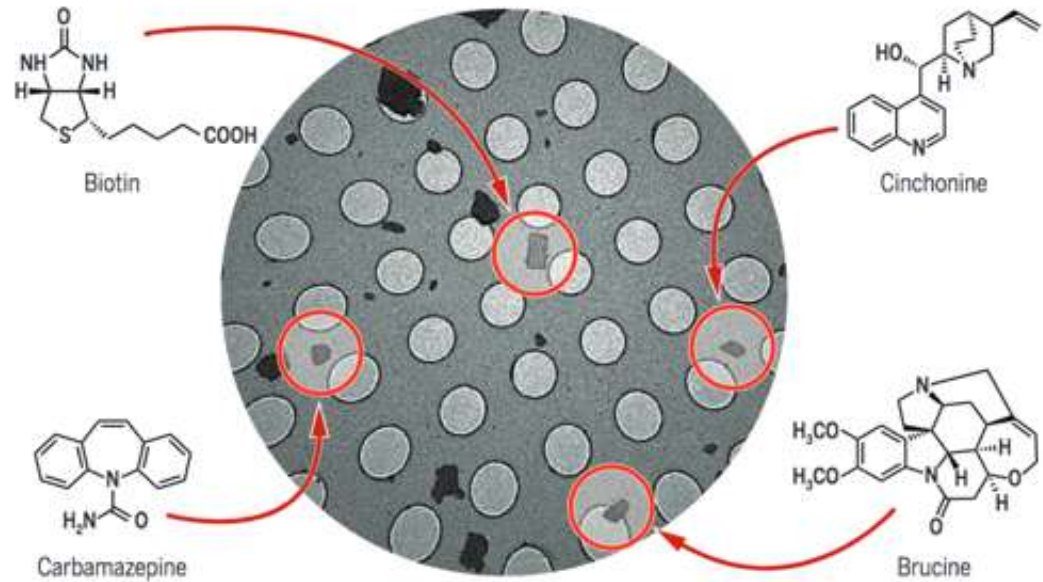
Structures can now be gleaned from micrometer-size crystals (black), seen here on an electron microscope slide. (GONEN LAB)

MicroED

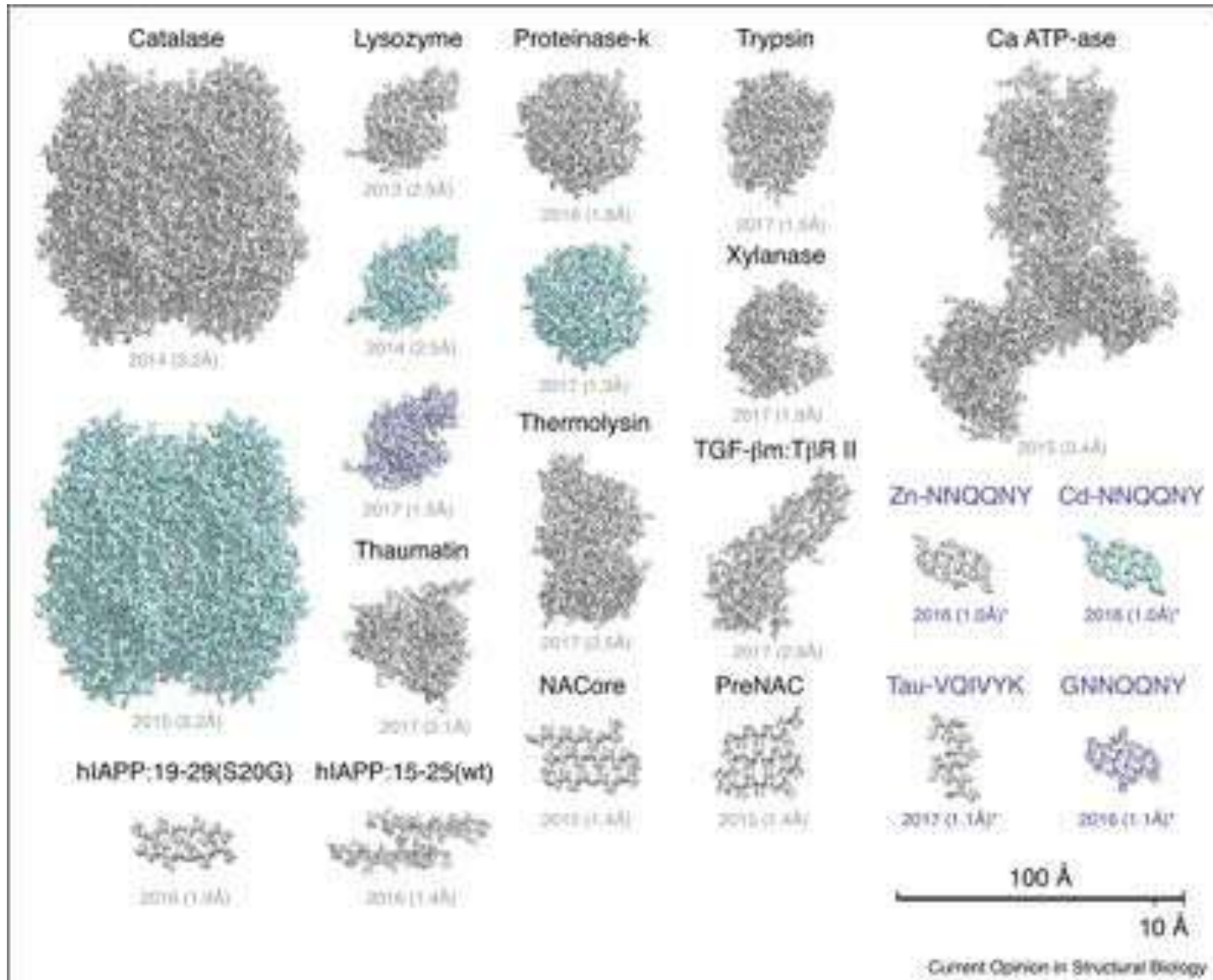
Runner-up for Science's 2018 Breakthrough of the Year

Structures from a mix of microcrystals

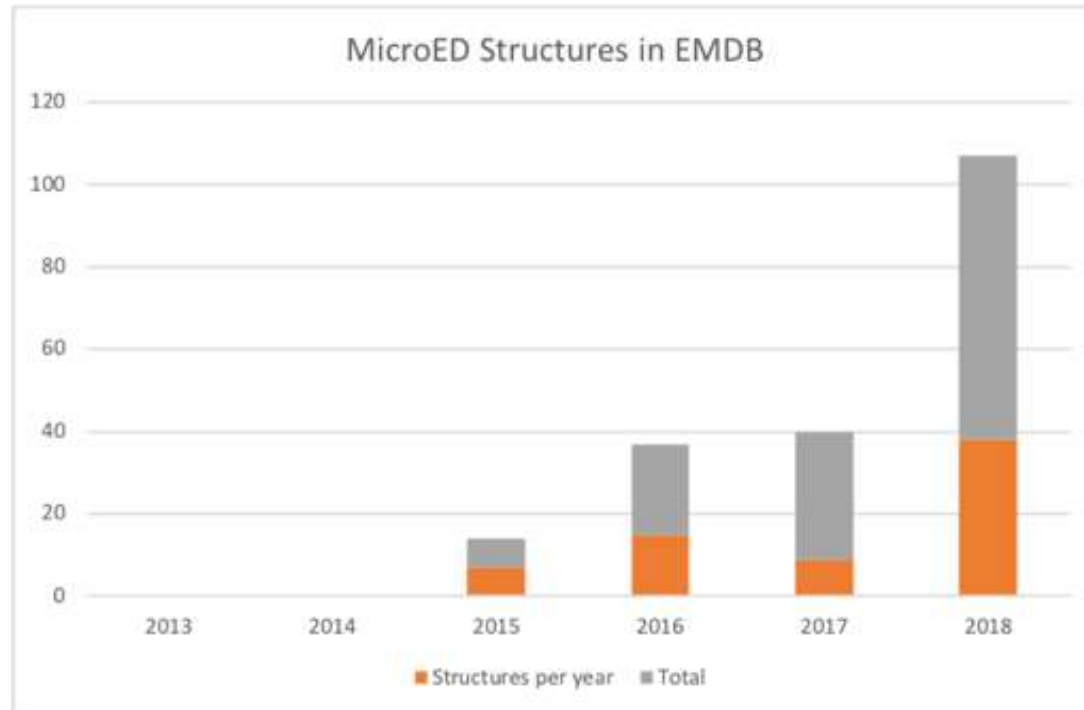
A new technique identified structures of four compounds from tiny crystals on an electron microscope slide.



Structures Solved by MicroED



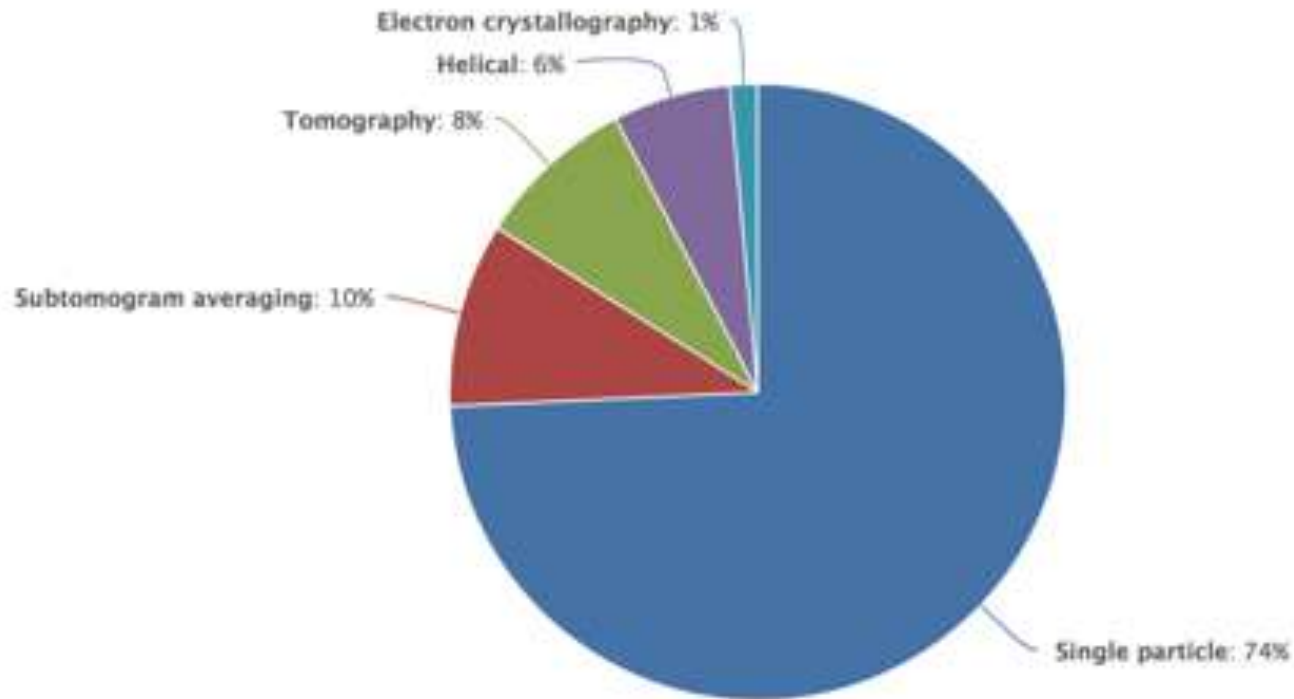
Structures Solved by MicroED (EMDB search)



| Year | Deposited Structures per year | Total Structures |
|------|-------------------------------|------------------|
| 2013 | 0 | 0 |
| 2014 | 0 | 0 |
| 2015 | 7 | 7 |
| 2016 | 15 | 22 |
| 2017 | 9 | 31 |
| 2018 | 38 | 69 |

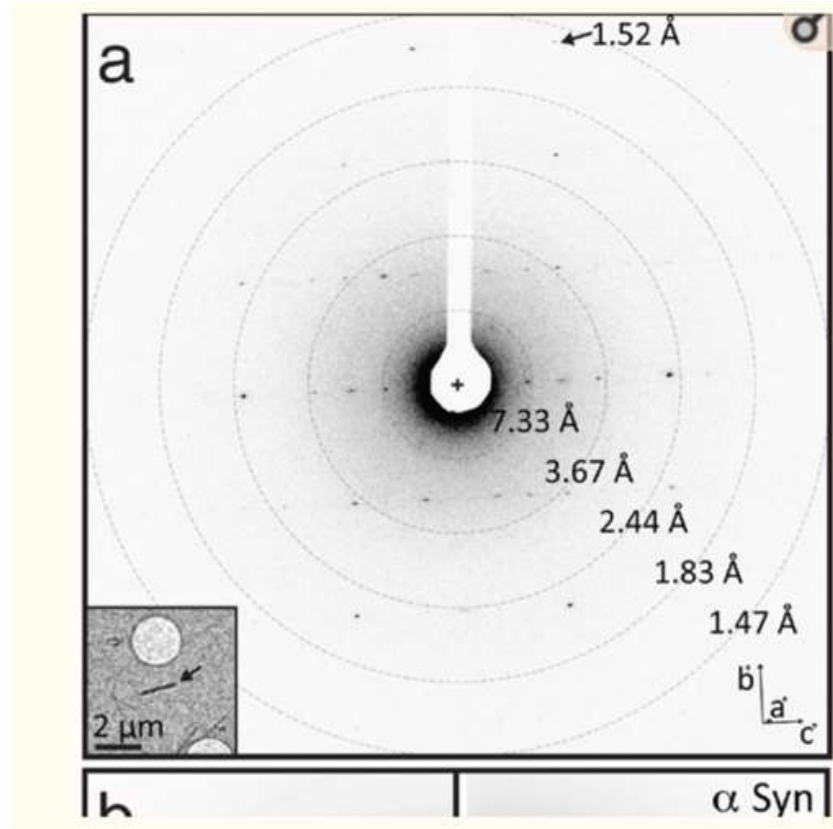
EMDB Statistics

Distribution of released maps (7780 in total) as a function of technique used

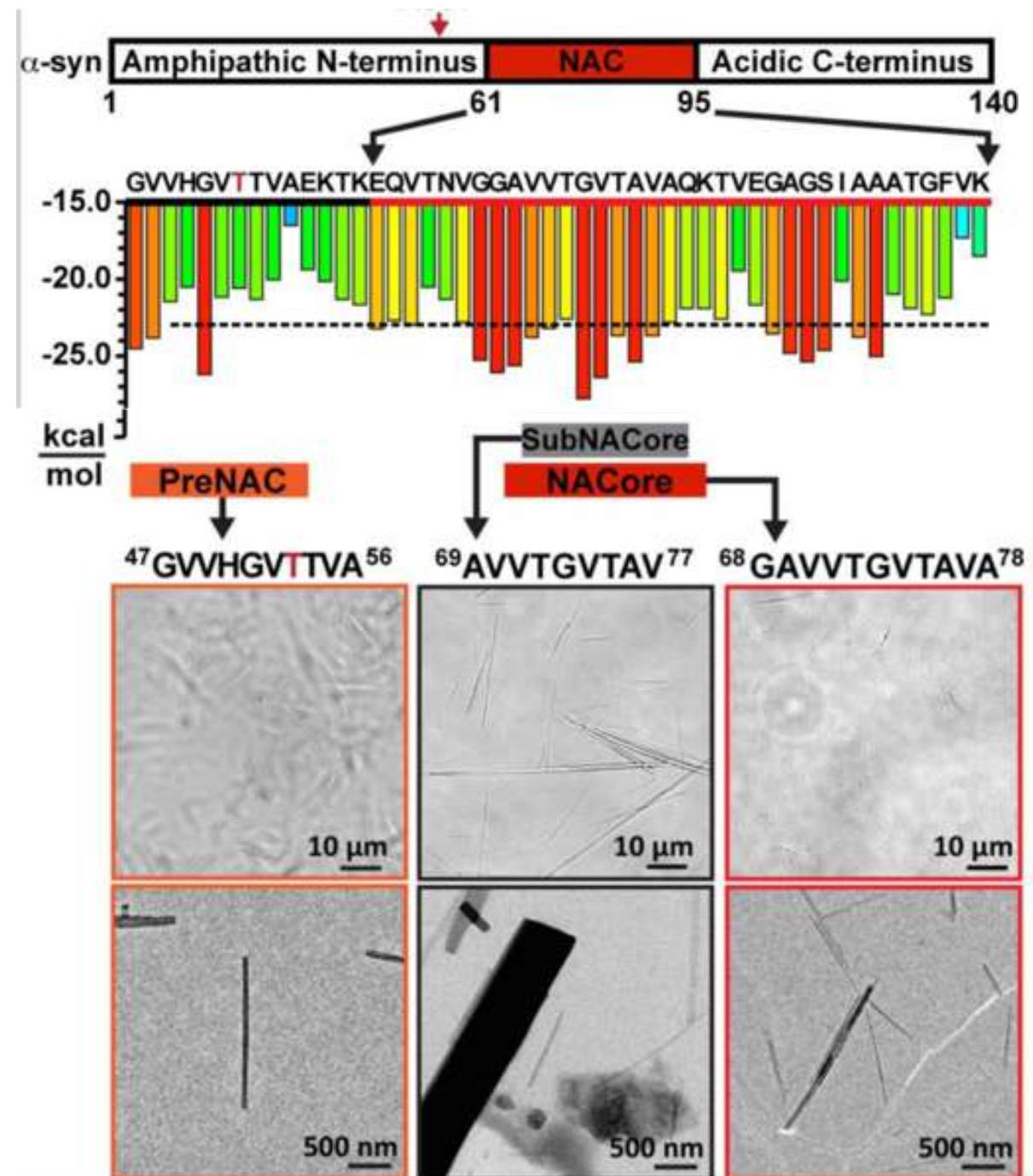


69/115 by MicroED
32 of these <1 kDa

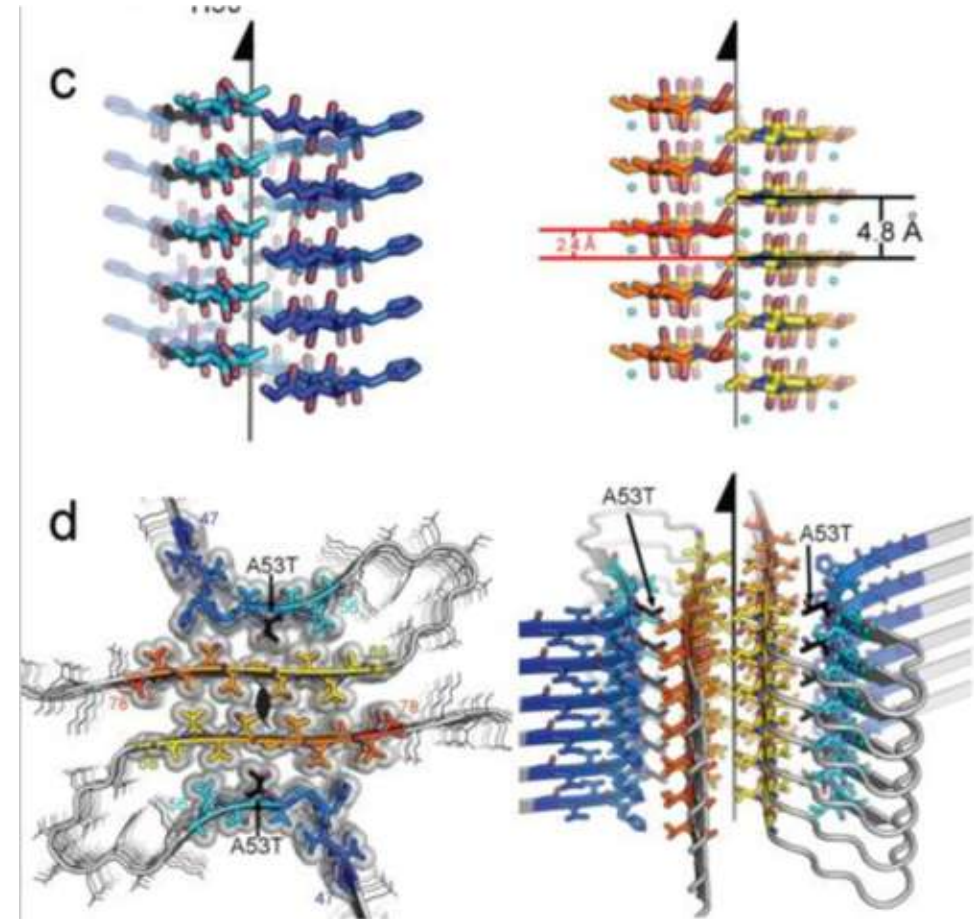
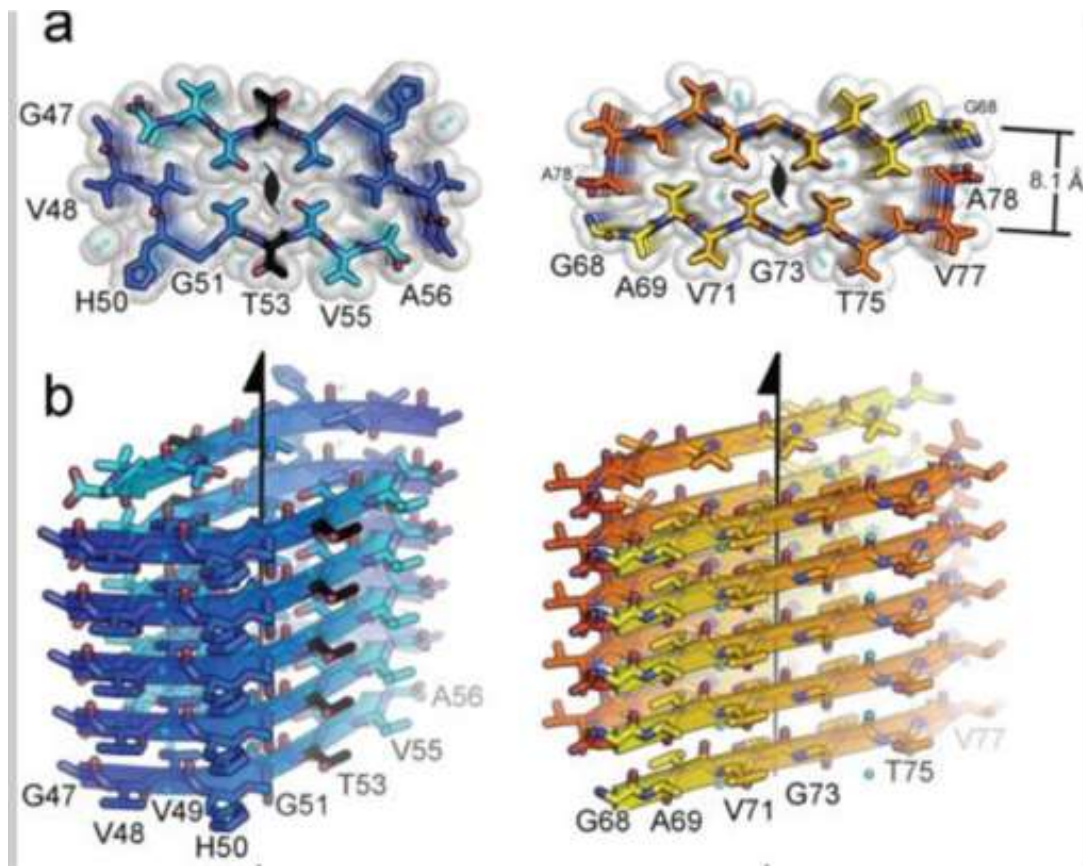
Toxic core of α -synuclein from invisible crystals



Rodriguez et al, 2015



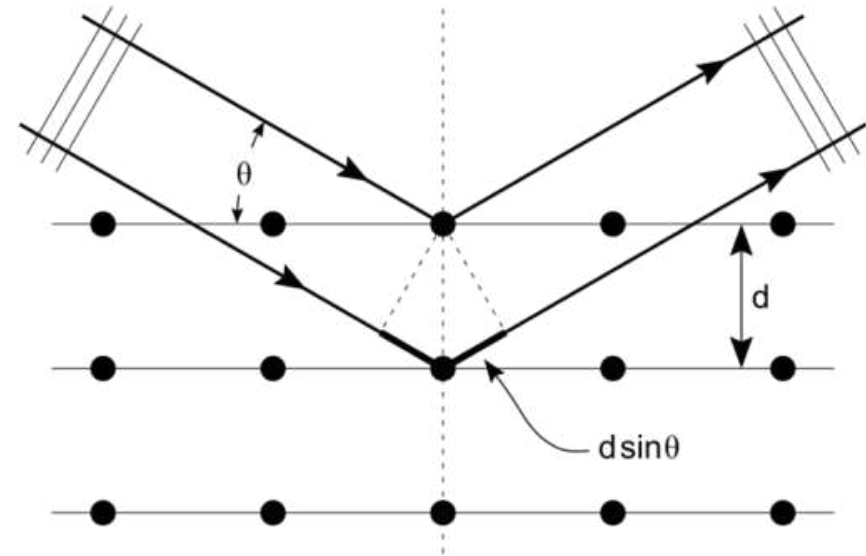
Structure of Amyloid core



Brief review of X-ray crystallography

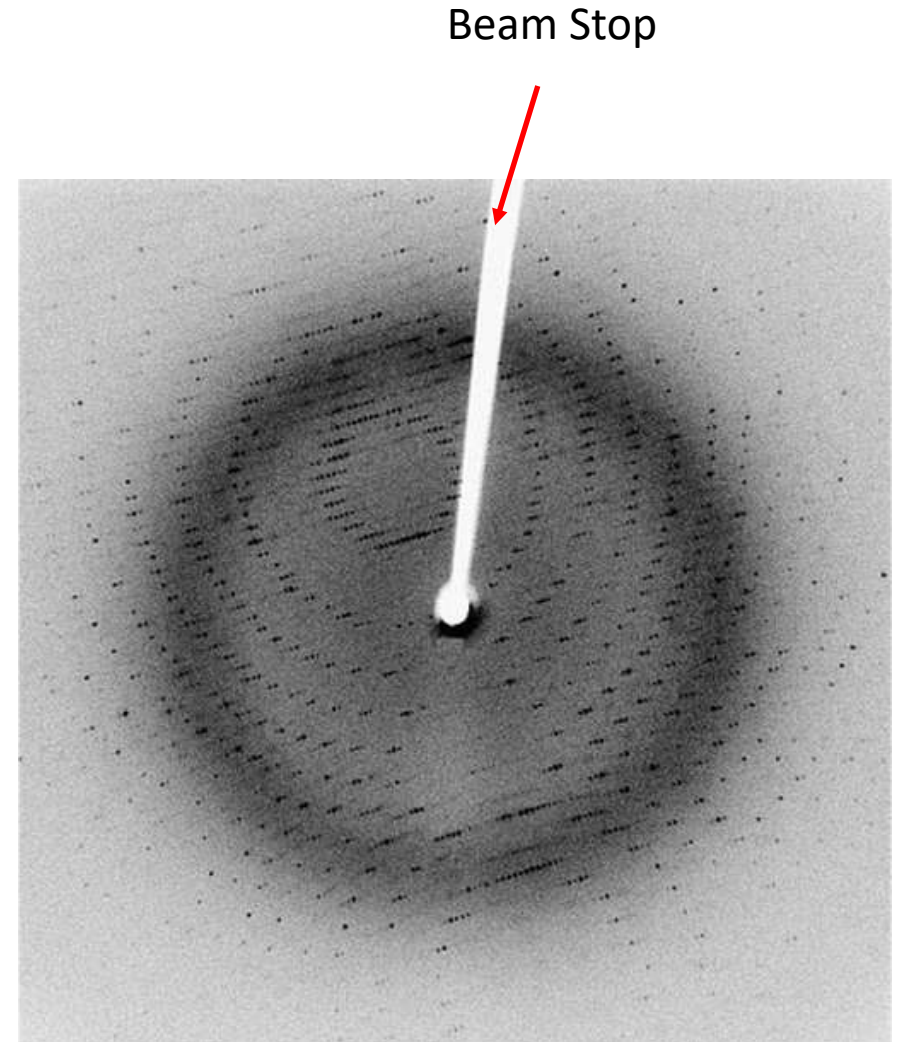
Diffraction Review

- Set of scattering points separated by distance d
- Beam hits at angle θ relative to plane
- Constructive interference only when their path length difference keeps them in phase
- Bragg's law
 - $n\lambda = 2d \sin \theta$
- Only one scattering event, does not deal with multiple scattering

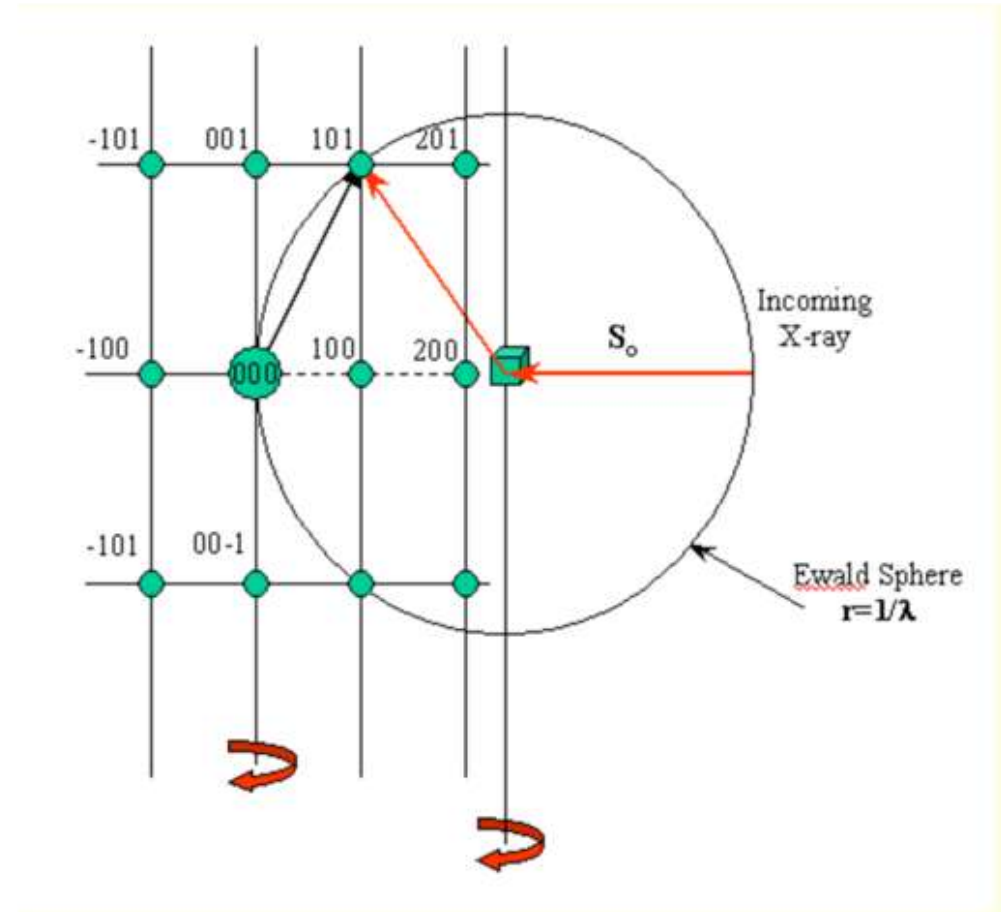
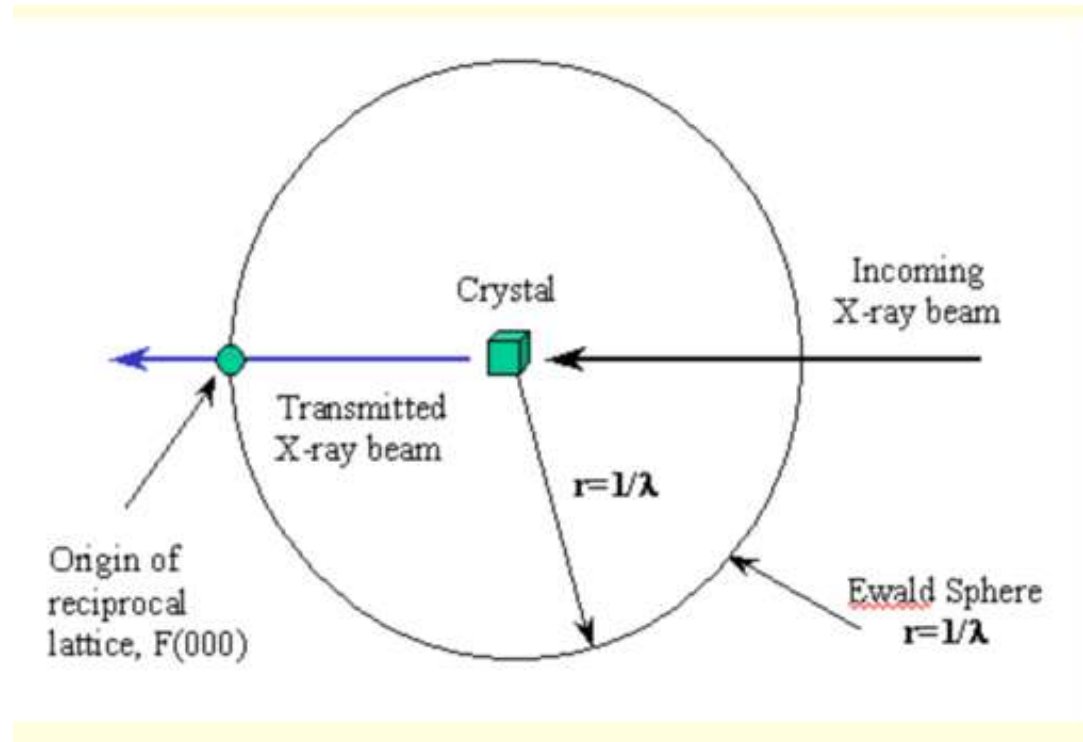


X-Ray Diffraction

- Mount crystal, expose to x-ray beam at defined wavelength
- Collect images of reflections on detector
- Only collect intensities and positions, not phases
- Rotate crystal (180 deg) to get all reflections
- From positions, get 3D lattice parameters
- Phasing
 - Ab initio (small, high resolution)
 - Heavy atom derivatives
 - MAD/SAD
 - Molecular replacement

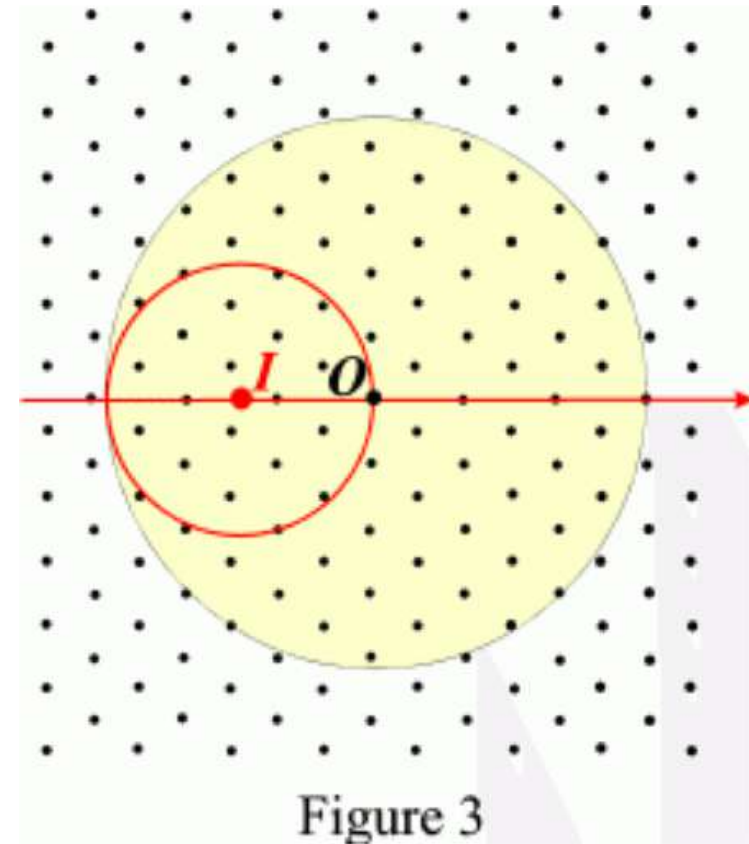


Ewald Sphere



Ewald Sphere

- If you rotate the crystal, the sphere rotates about the origin O
- Yellow area is swept out
- Only observe reflections in the yellow area



Limitations of X-ray crystallography

- Approximately 30% of proteins that crystallize do not produce crystals large enough for x-ray diffraction experiments
 - Rupp, 2004; Quevillon-Cheruel et al., 2004
- XFEL?
 - Need many crystals
 - Expensive experiment

Wavelengths

- X-ray
 - $\lambda=70.9$ pm (Ag Ka)
 - $\lambda =154$ pm (Cu Ka)
- EM
 - 80 keV: 4.18 pm
 - 120 keV: 3.35 pm
 - 200 keV: 2.51 pm
 - 300 keV: 1.97 pm

Three-dimensional electron crystallography of protein microcrystals.

Elife 2013 Nov 19

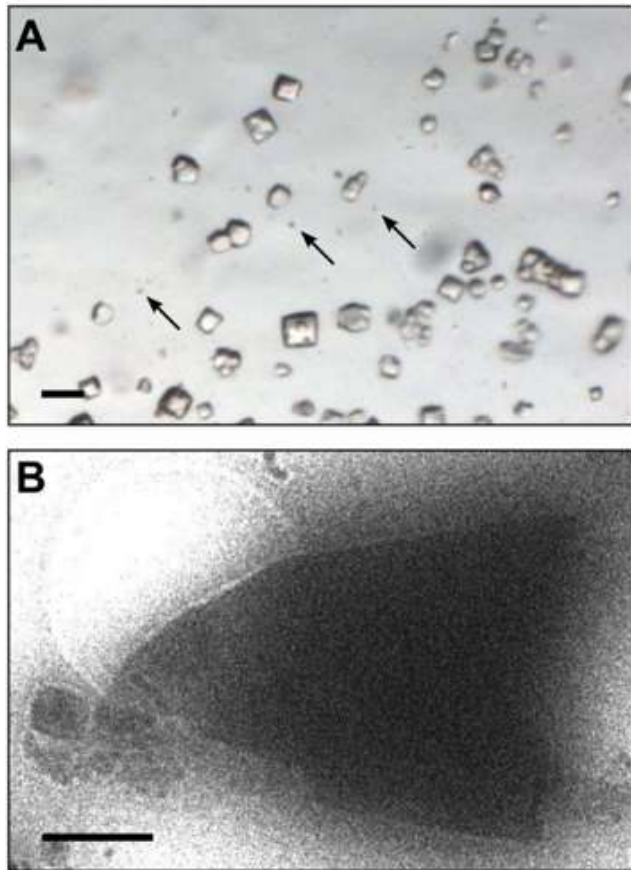


Figure 1. Images of lysozyme microcrystals. **(A)** Light micrograph showing lysozyme microcrystals (three examples indicated by arrows) in comparison with larger crystals of the size normally used for X-ray crystallography. Scale bar is 50 μm . **(B)** Lysozyme microcrystals visualized in over-focused diffraction mode on the cryo-EM prior to data collection. The length and width of the crystals varied from 2 to 6 μm with an estimated thickness of $\sim 0.5\text{--}1\text{ }\mu\text{m}$. Scale bar is 1 μm .

DOI: [10.7554/eLife.01345.003](https://doi.org/10.7554/eLife.01345.003)

Original implementation (Shi et al, 2013)

- Image single images at various tilts (1 deg increment)
 - Oscillation generally used in x-ray crystallography
- Reflections recorded in this manner are generally partial reflections
 - Needed in-house scripts to index the data and group symmetry-related reflections
- Lysozyme at 2.9 Å resolution
 - 200 keV on TVIPS F416 CMOS detector

Critical Dose for Diffraction Imaging

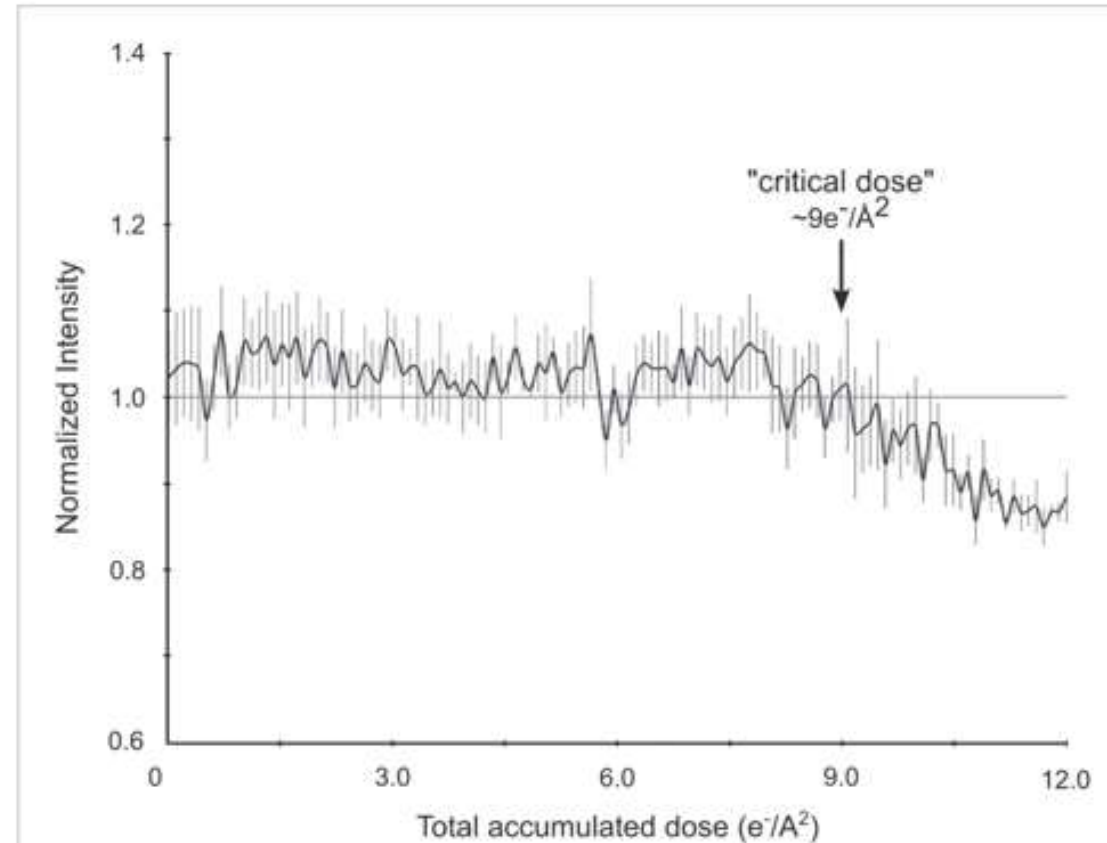


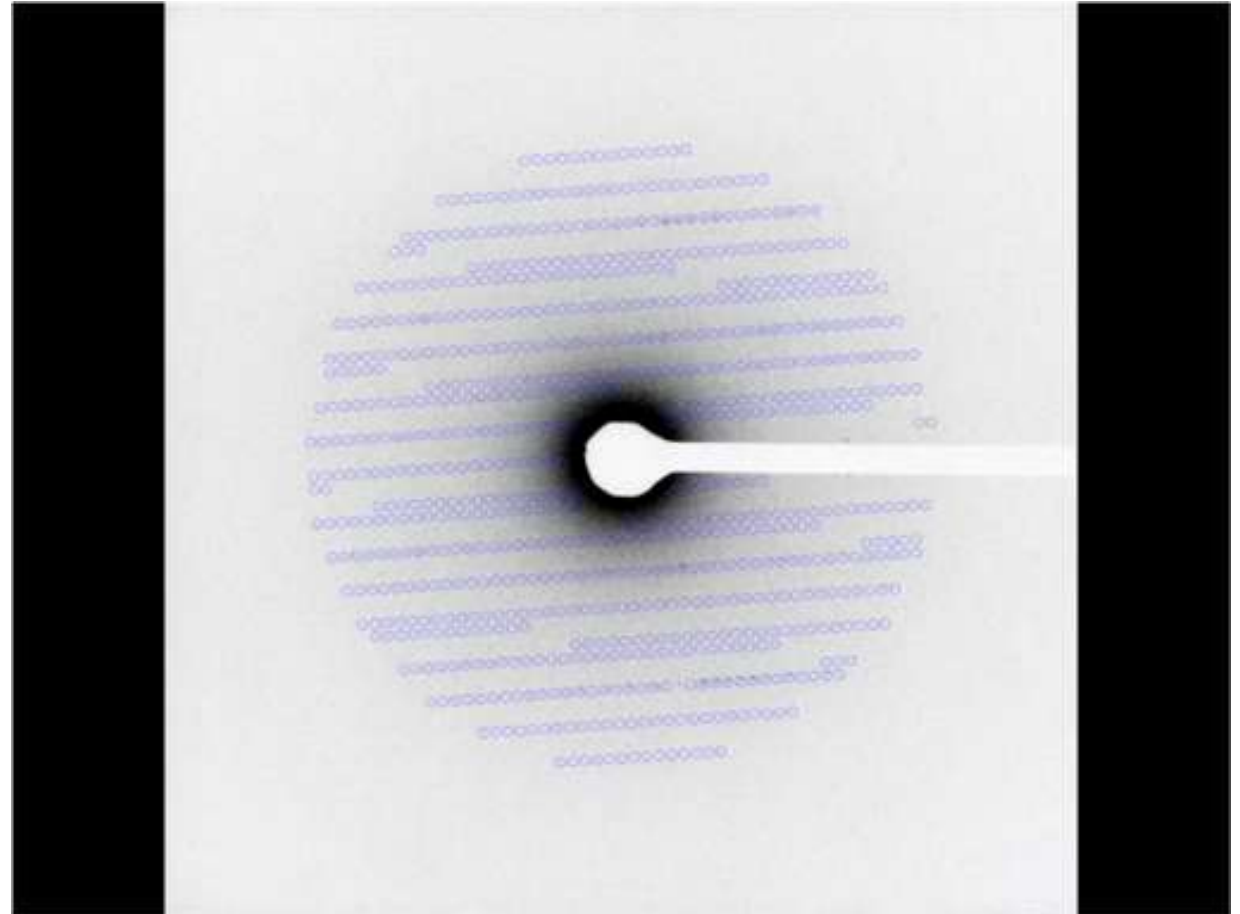
Figure 3. Effects of cumulative electron dose on diffraction data quality. A single lysozyme microcrystal was subjected to 120 sequential exposures without tilting, each of a dose of $\sim 0.1 \text{ e}^-/\text{\AA}^2$ for a total accumulated dose of $\sim 12 \text{ e}^-/\text{\AA}^2$. Normalized intensity vs total accumulated dose for three diffraction spots observed over all 120 sequential frames was plotted. A decrease in diffraction intensity becomes apparent at a dosage of $\sim 9 \text{ e}^-/\text{\AA}^2$ ('critical dose'). Bars represent standard error of the mean.

DOI: [10.7554/eLife.01345.005](https://doi.org/10.7554/eLife.01345.005)

Diffraction from single crystal

Video 1. An example of a complete three-dimensional electron diffraction data set from a single lysozyme microcrystal. In this example, diffraction patterns were recorded at 1° intervals from a single crystal, tilted over 47°. Cumulative dose was $\sim 5 \text{ e}^-/\text{\AA}^2$ in this example.

[DOI: 10.7554/eLife.01345.006](https://doi.org/10.7554/eLife.01345.006)



Small changes in tilt alter intensity

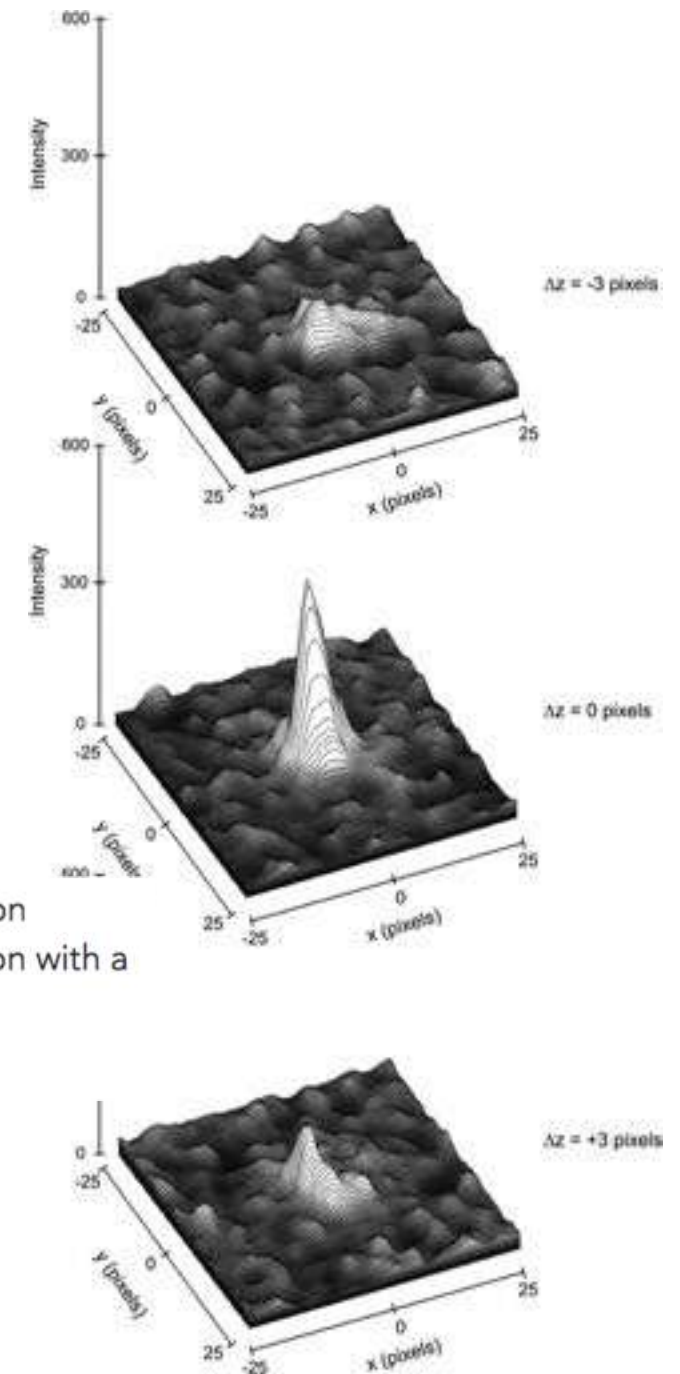


Figure 5. Three-dimensional profiles of the intensity of a single reflection over three consecutive diffraction patterns at -0.1° , 0° , and 0.1° degree tilts. The plots show the approximate dimensions of the full reflection with a width (full width at half maximum height) of 3–5 pixels in the x, y, and z direction.

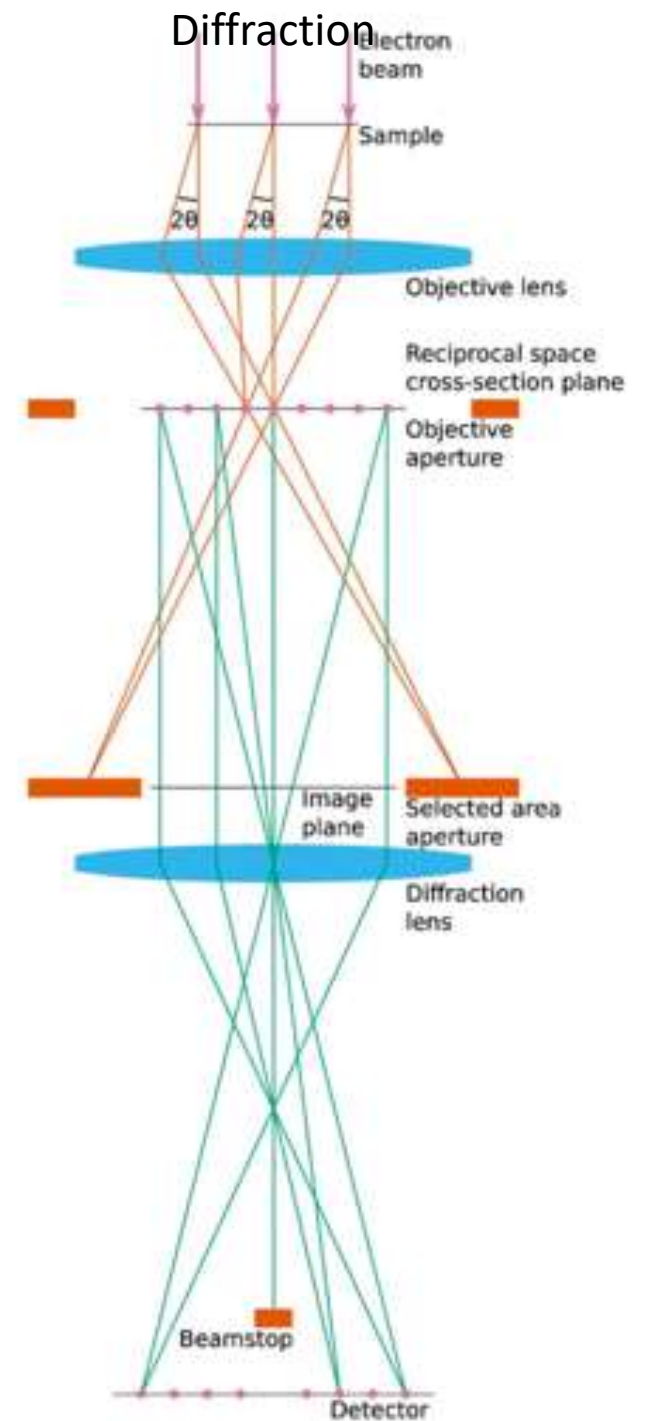
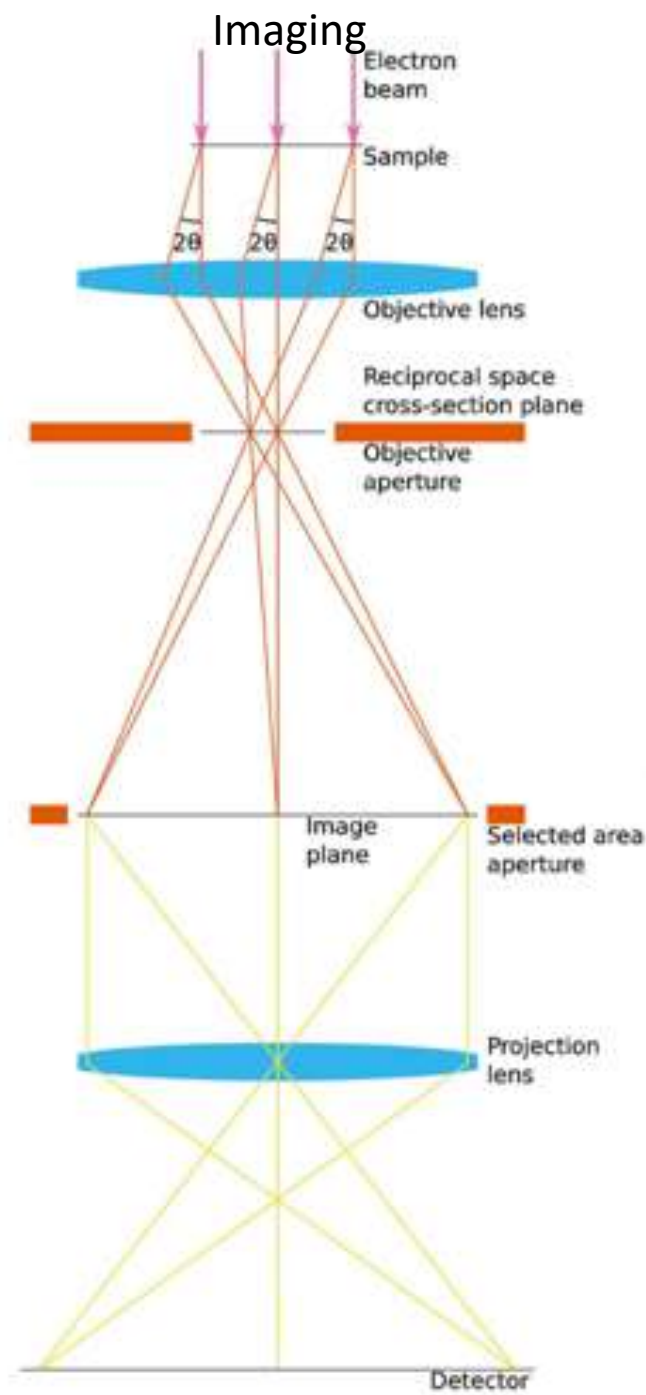
DOI: [10.7554/eLife.01345.009](https://doi.org/10.7554/eLife.01345.009)

Better Data Collection: Continuous rotation

- Rotate stage at continuous rate
- Rotate to coordinate with exposure time
- Camera needs to be in continuous “rolling shutter” mode
- High rotation rate: increases the recorded reflection fraction on each frame
 - Too high: spot overlap
- Low rotation rate: makes weaker, high resolution reflections more visible
 - Too low: too few spots per image

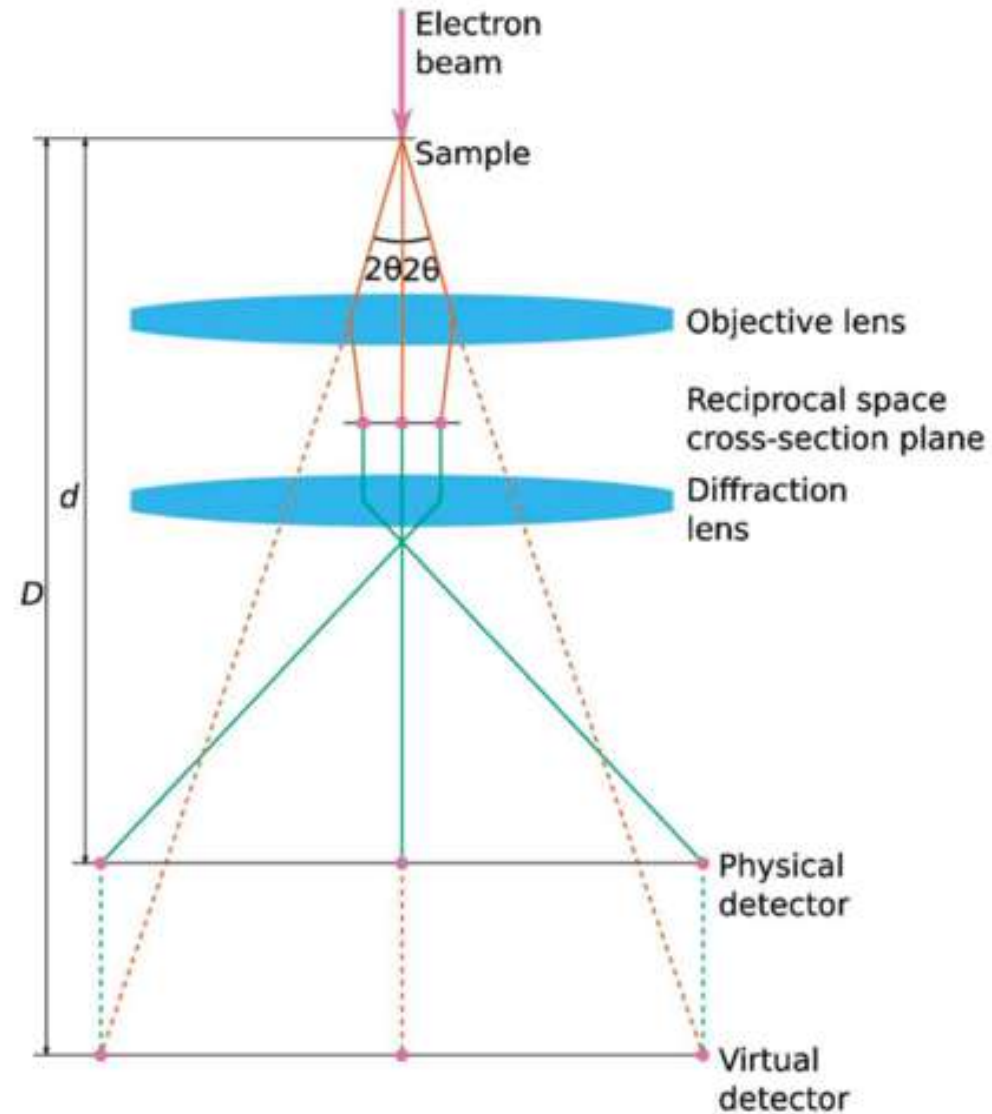
Electron microscope setup for diffraction

Electron Optics



Electron Optics

Camera length can be changed



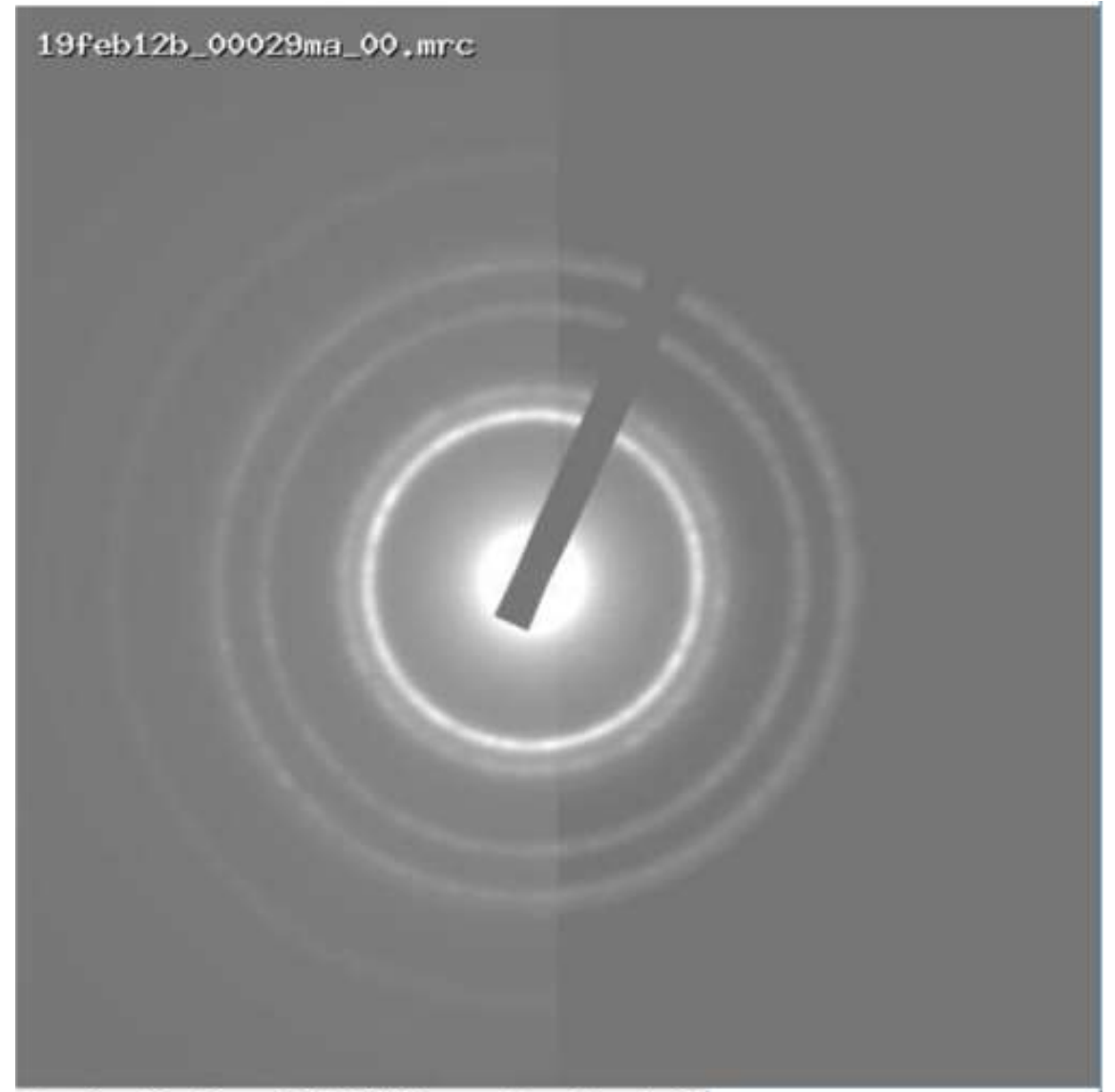
Diffraction data

- Not affected by
 - Stage instabilities
 - Beam induced specimen movement, charging
 - Optical aberrations (CTF: defocus, astigmatism, Cs,...)
 - Except: diffraction astigmatism
 - Temperature instabilities
- Only intensities (amplitude²) collected
 - Phase problem

Gold Diffraction on JEOL 1230

80 keV

Outer ring: 1.2 Å resolution



Diffraction and beam stop alignment

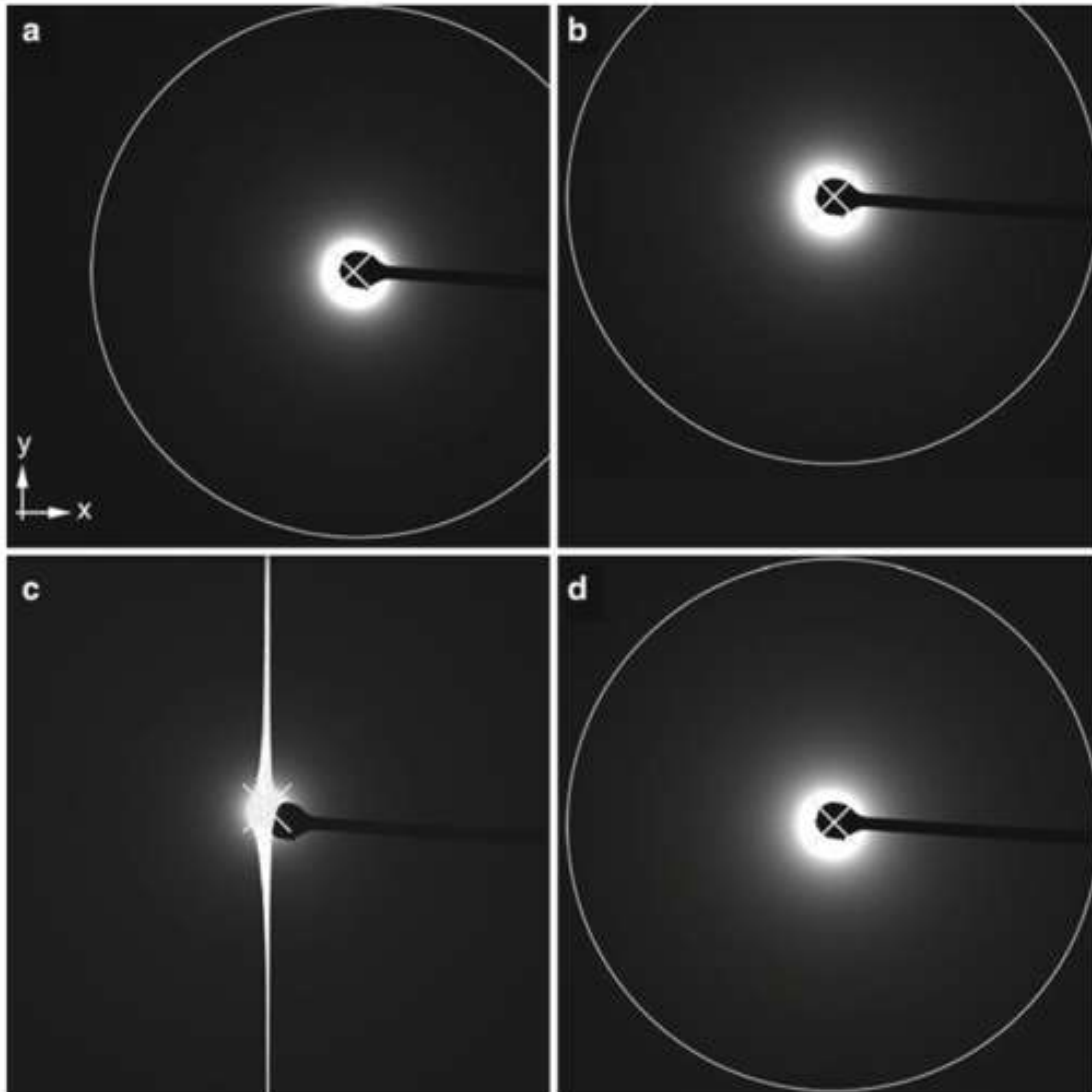
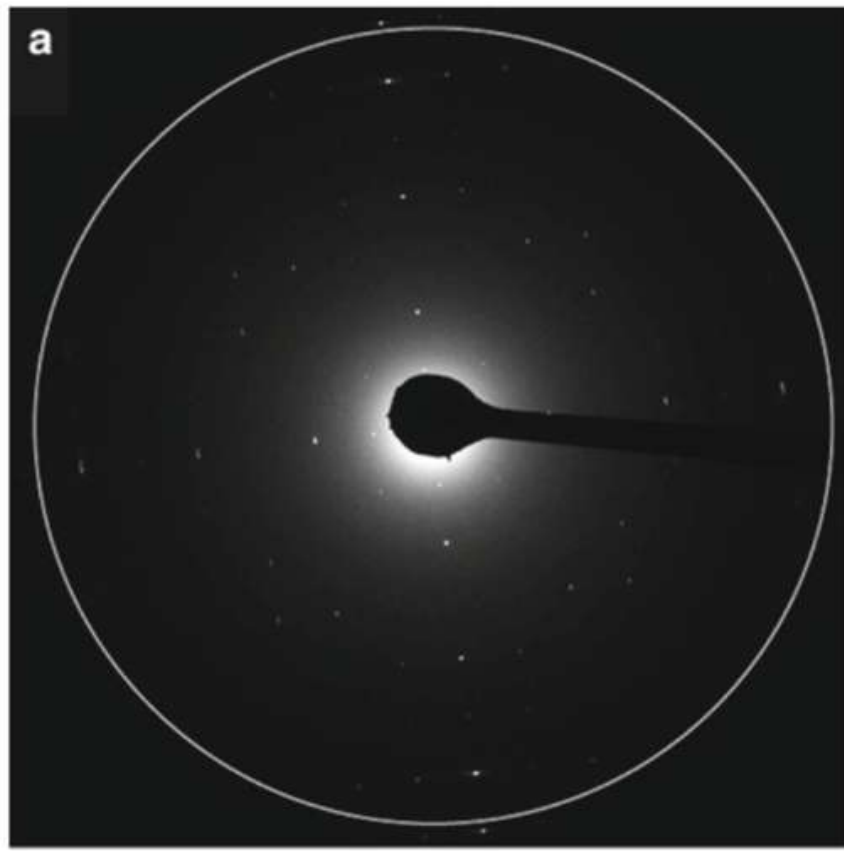
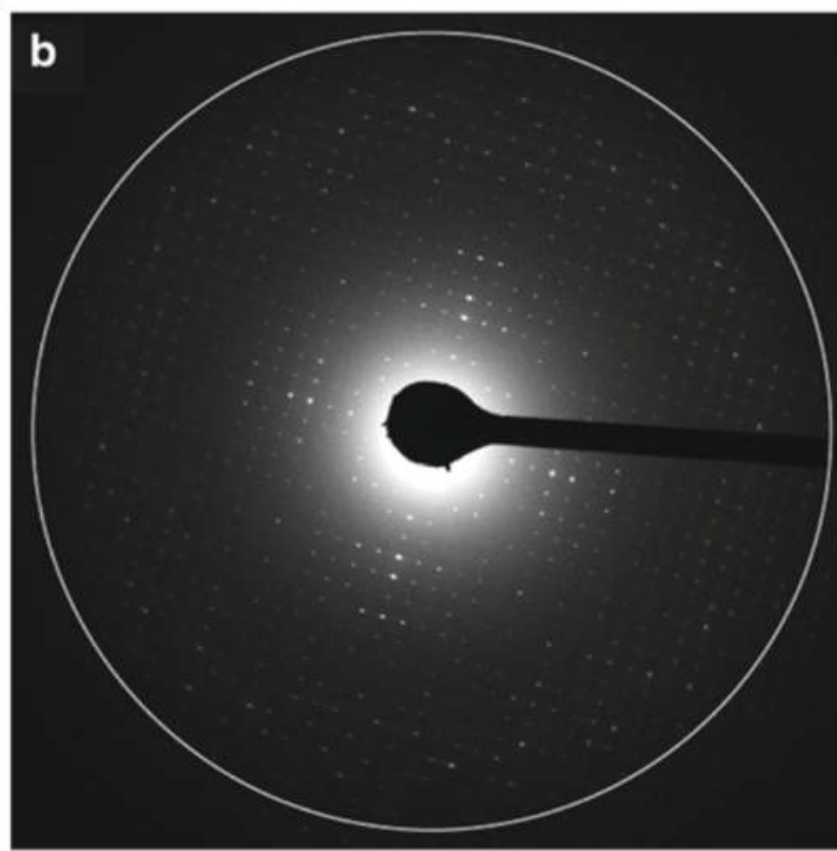


Fig. 5. Alignment of the beam with the beam stop and with the CCD. It is important to align all three elements well; the beam must be at the center of the recordable area of the CCD so that no information will be lost, and the beam stop must be aligned with the beam to prevent damage to the CCD. (a and b) An example of a beam (indicated by an "x") that is well aligned with the beam stop. The beam, however, is not at the center of the recordable area of the CCD and information on the x-axis or the y-axis is lost (a and b, respectively). (c) An example where the beam is aligned roughly at the center of the recordable area of the CCD but is not aligned with the beam stop. As a result the CCD is oversaturated and bleed-through in the y-axis is observed. (d) Perfect alignment. The beam is at the center of the recordable area of the CCD and directly behind the beam stop. Data to the same resolution can be recorded in all directions as indicated by the circle. In all panels the white X marks the center of the beam.

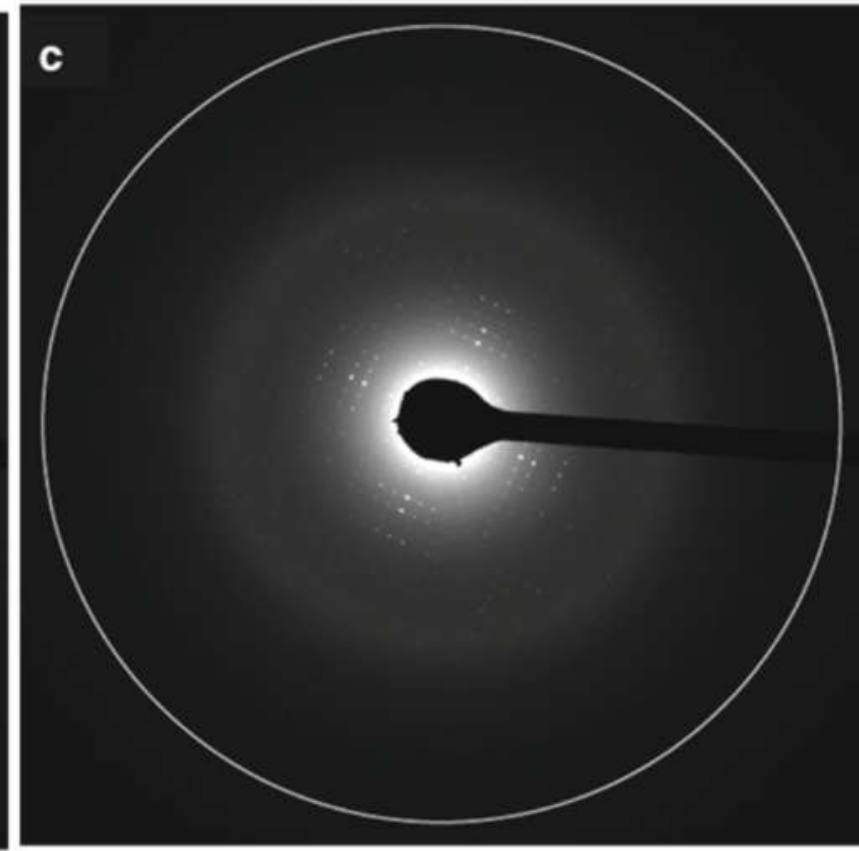
Selection and calibration of diffraction length



4,000 mm
10 Å at edge

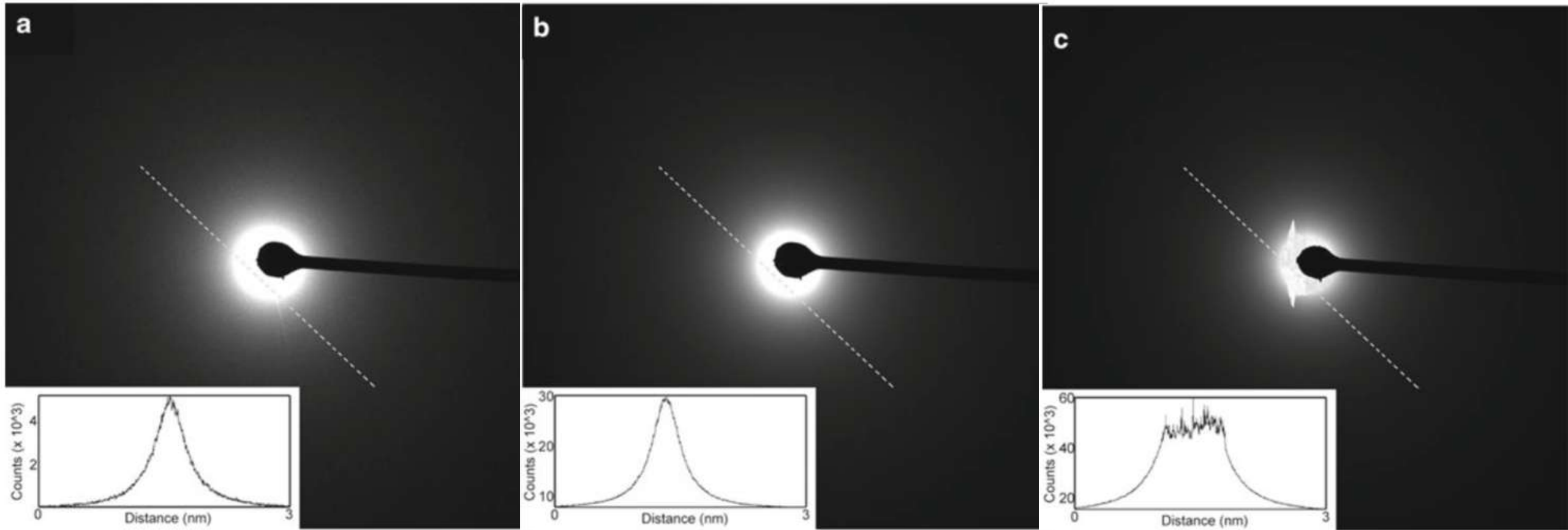


3,000 mm
3 Å at edge



1,750 mm
1.5 Å at edge

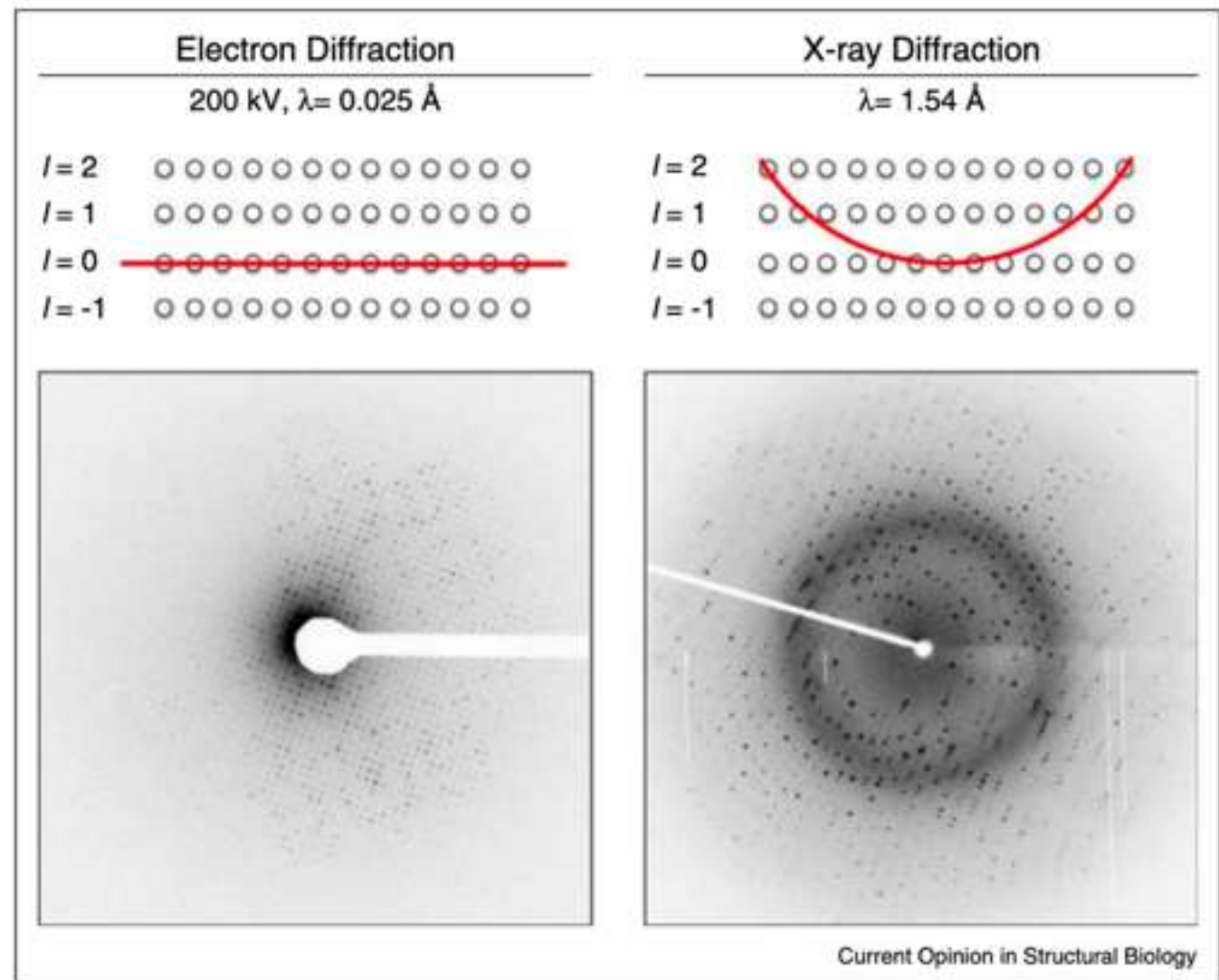
Exposure Time: too short (undersaturated),
too long (oversaturated)



Standard setup for single particle imaging

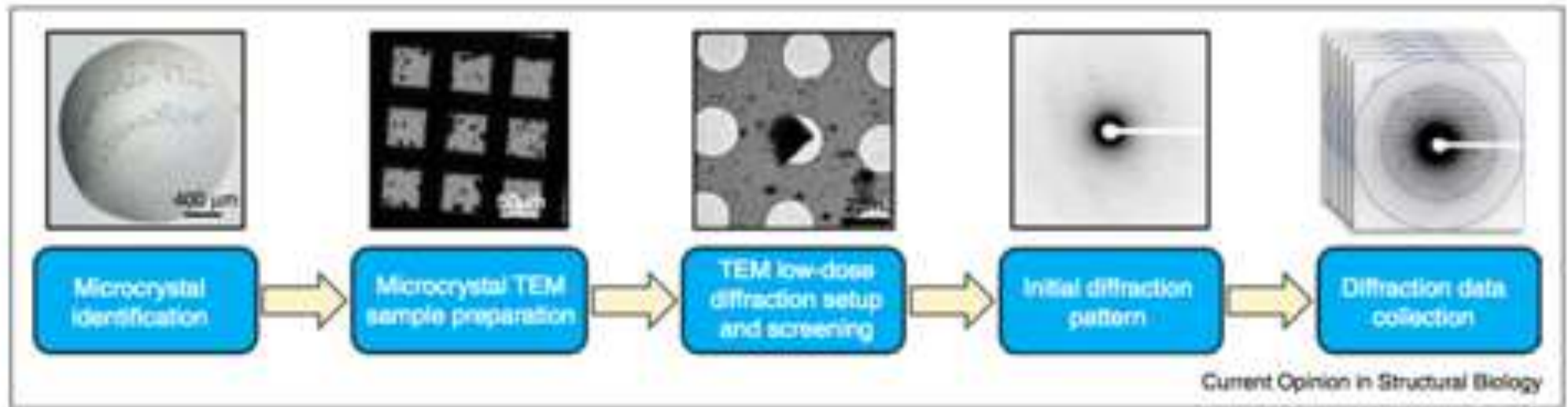
- Adjust optics to minimize aberrations:
 - Astigmatism
 - beam tilt (coma)
- Define area away from sample for focus determination (image-beam shift)
- Define image-beam shift pattern for imaging
- Choose a range of defocus values to fill in the CTF of the dataset
- Automate to collect thousands of images

Ewald Sphere



Comparison of diffraction data obtained from lysozyme crystals by electron diffraction and X-ray diffraction. Because the wavelength of the diffracting electrons is so short, the resulting Ewald sphere (left, red line) is essentially a plane when compared to the Ewald sphere for X-ray diffraction (right, red line). Diffraction only occurs when the Ewald sphere contacts a reflection in reciprocal space (top panels, white circles represent reflections in reciprocal space). Therefore, because the Ewald sphere is so flat, the patterns produced from electron diffraction (bottom left) appear as planar 2-dimensional slices through the 3-dimensional volume of reflections, whereas the patterns from X-ray diffraction (bottom right) appear as circular 2-dimensional projections of the sphere on the detector.

Workflow Overview



Screening

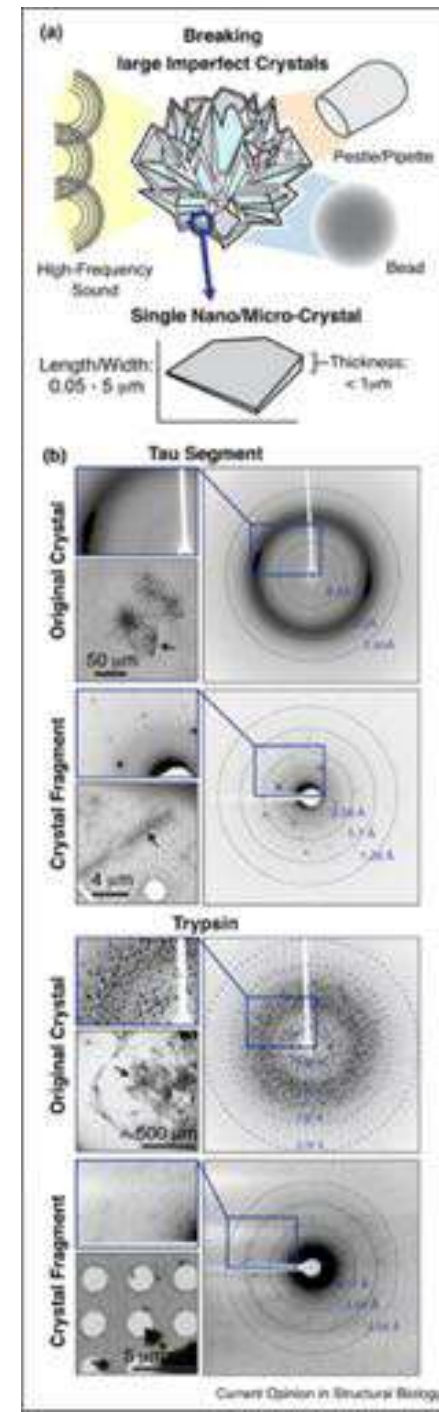
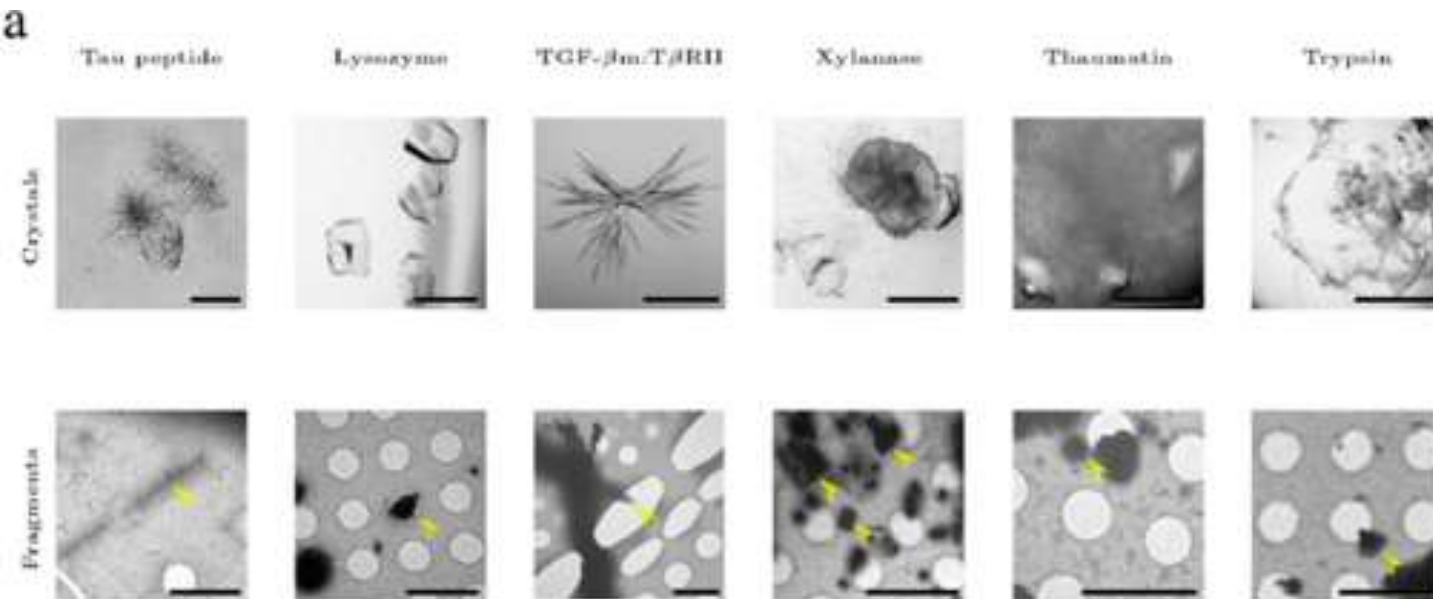
- Use traditional setup for X-ray crystallography
- Cloudy drops
 - Upper limit for thickness: 400 nm (practical limit), thinner is better
- Negative stain screening for crystals
 - Side entry holders make large scale cryo screening difficult
 - Can screen much more quickly with autoloaders (12 at a time) but \$20 per grid
- Initial screen
 - Low mag (100x), $<10^{-6}$ e/Å²/s
 - Survey grid, find crystal-containing areas
 - Screen more finely in overfocused diffraction mode
 - Low dose $<10^{-3}$ e/Å²/s

Crystal Thickness

- Diffuse scattering: caused by partial disorder within crystal, as well as inelastic scattering
 - Increased background noise, errors in measurement of intensity levels
- Dynamic scattering: when inelastically scattered electrons have a second scattering effect
 - Intensities meant for a specific reflection are redistributed to other ones, leading to inaccuracies of integrated reflection counts
- Lysozyme: crystals thicker than 500 nm unusable
 - Maximum thickness may depend on packing and density

Larger (imperfect) crystals

→ Break them up



Nannenga and Gonen, 2014
de la Cruz et al, 2017

Thick Crystals

All rights reserved. No reuse allowed without permission.

Collection of continuous rotation MicroED Data from Ion Beam Milled Crystals of Any Size

Michael W. Martynowycz,^{1,2} Wei Zhao,³ Johan Hattne,^{1,2} Grant J. Jensen,^{3,4} and Tamir Gonen,^{1,2,5,*}

¹ Howard Hughes Medical Institute, University of California, Los Angeles, Los Angeles, CA

² Department of Biological Chemistry, University of California, Los Angeles, Los Angeles, CA

³ Department of Biology and Biological Engineering, California Institute of Technology, Pasadena, CA

⁴ Howard Hughes Medical Institute, California Institute of Technology, Pasadena, CA

⁵ Department of Physiology, University of California, Los Angeles, Los Angeles, CA

* To whom correspondence should be sent: tgonen@ucla.edu

J Struct Biol, 2019 Mar 1;205(3):59-64. doi: 10.1016/j.jsb.2019.02.004. Epub 2019 Feb 20.

Using focus ion beam to prepare crystal lamella for electron diffraction.

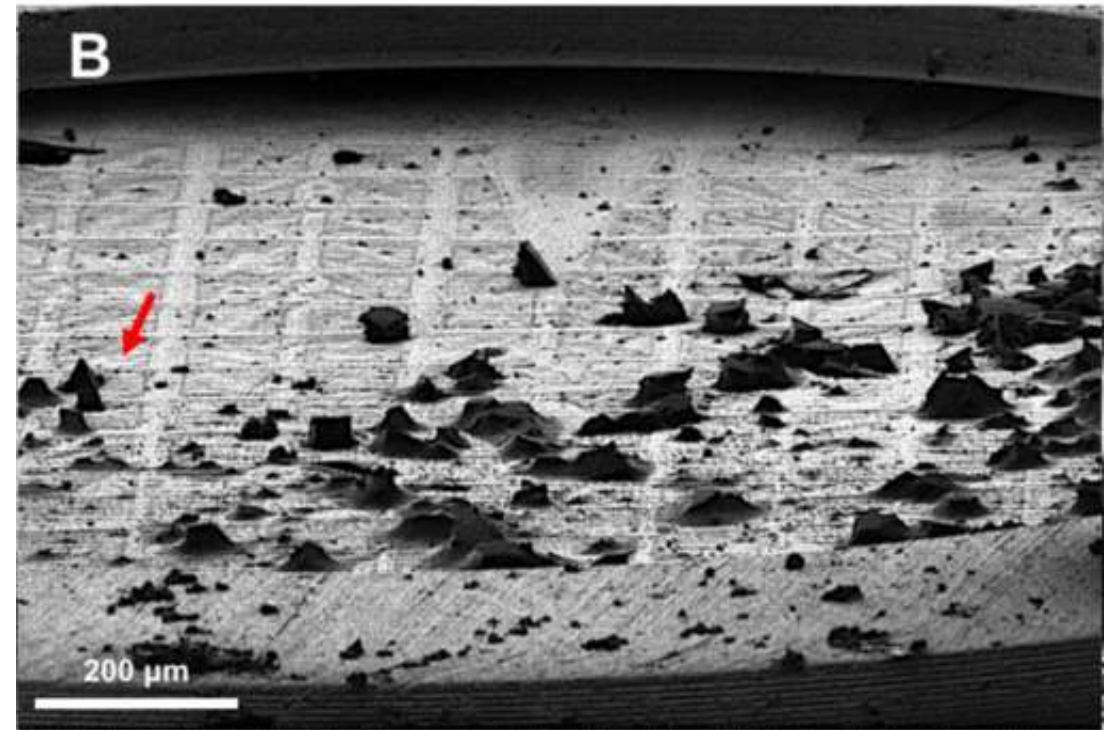
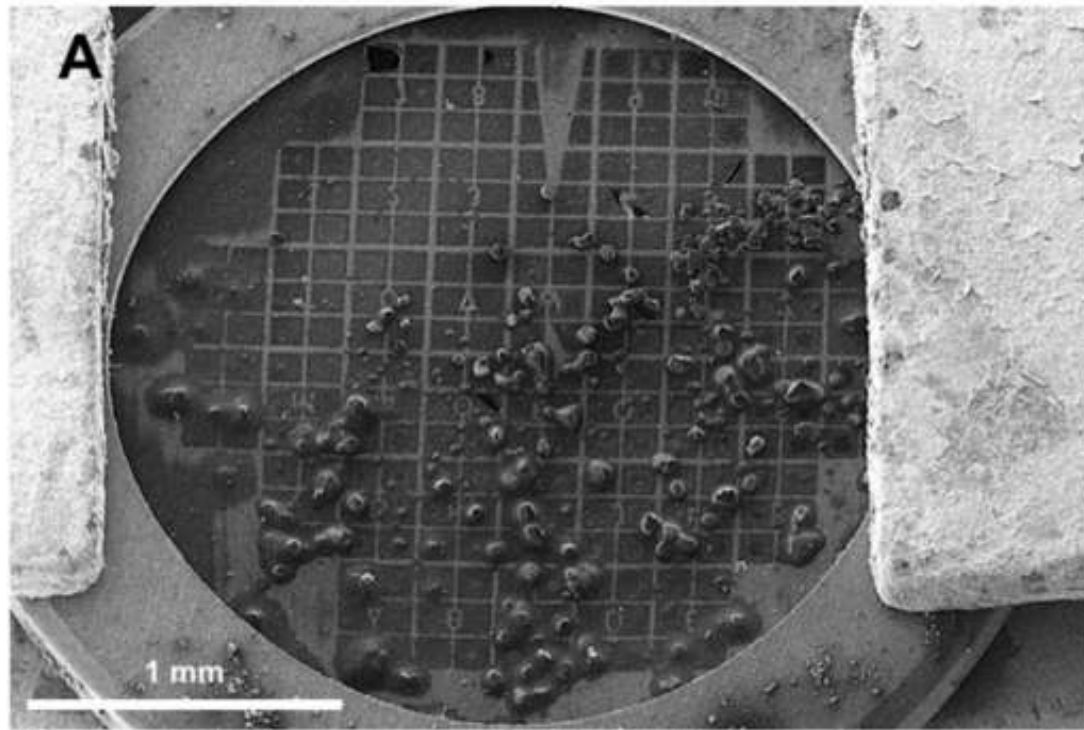
Zhou H¹, Luo Z¹, Li X².

Ⓢ Author information

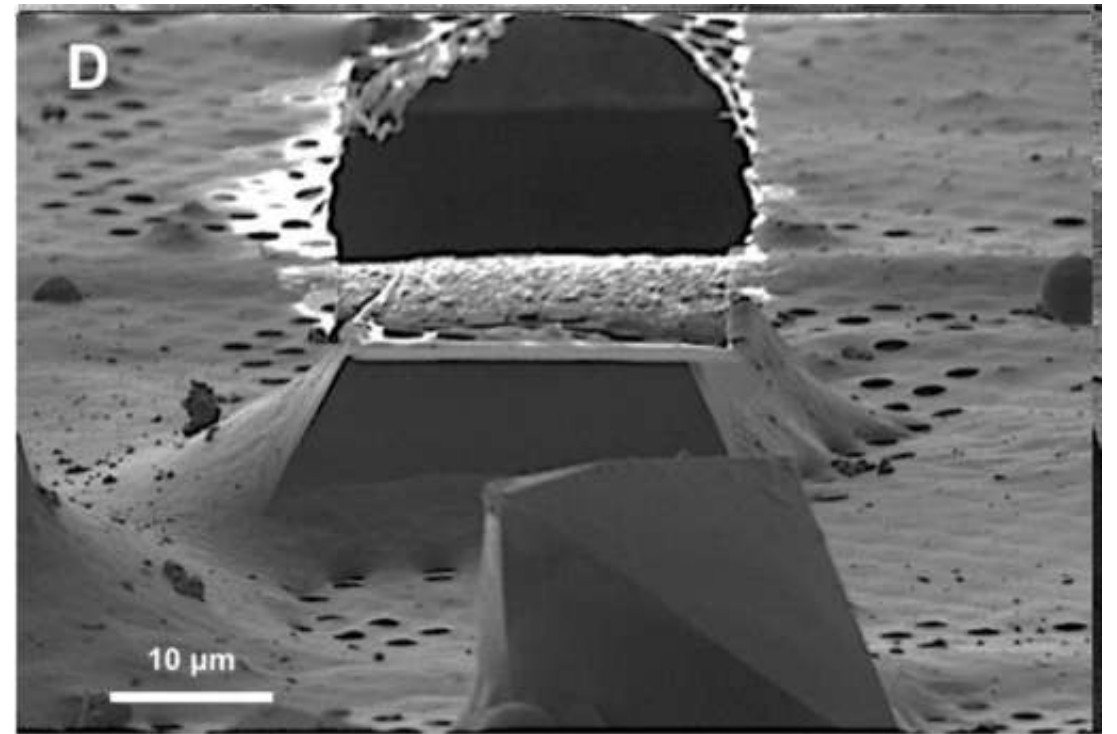
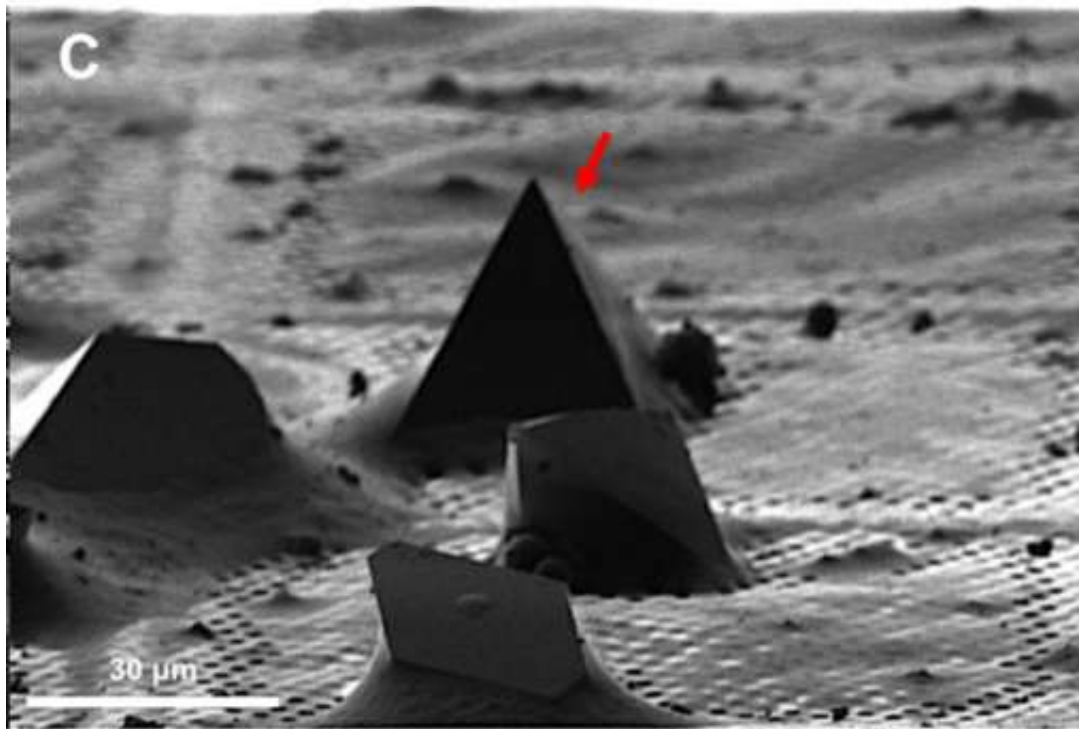
Abstract

Electron diffraction provides a powerful tool to solve the structures of small protein crystals. However, strong interactions between the electrons and the materials limit the application of the electron crystallographic method on large protein crystals with micrometer or larger sizes. Here, we used the focused ion beam (FIB) equipped on the scanning electron microscope (SEM) to mill a large crystal to thin lamella. The influences of the milling on the crystal lamella were observed and investigated, including radiation damage on the crystal surface during the FIB imaging, deformation of the thin crystal lamella, and variation in the diffraction intensities under electron radiation. These observations provide important information to optimize the FIB milling, and hence is important to obtain high-quality crystal samples for routine structure determination of protein crystals using the electron cryo-microscope.

Use a FIB to thin them

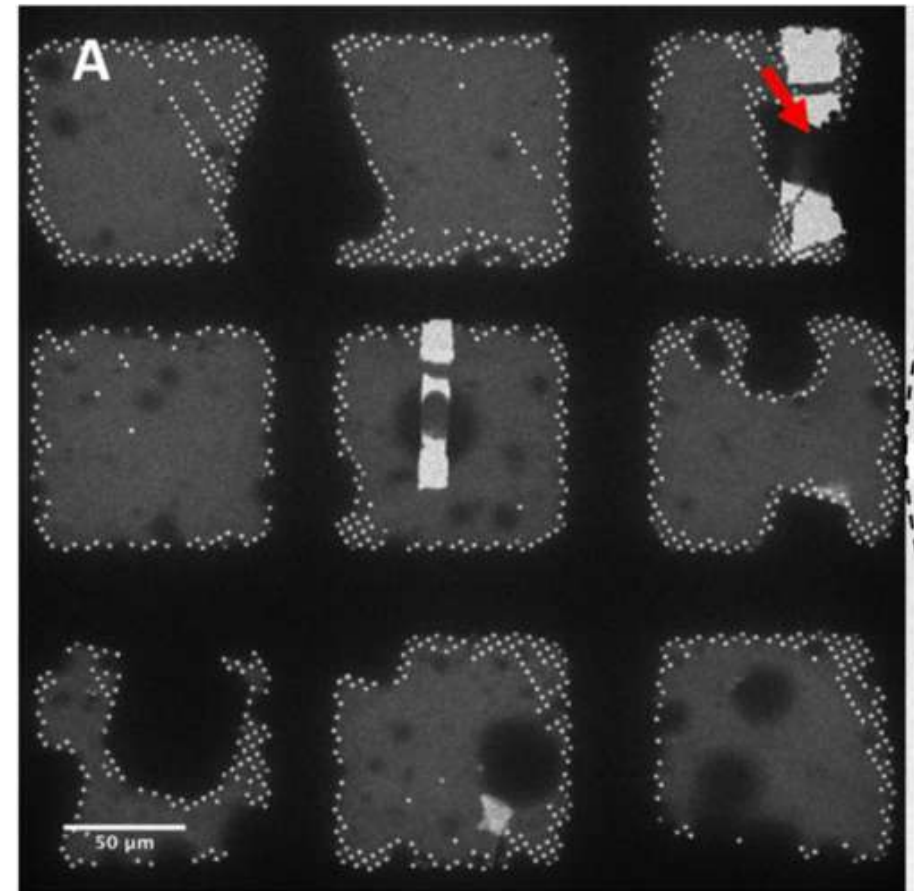
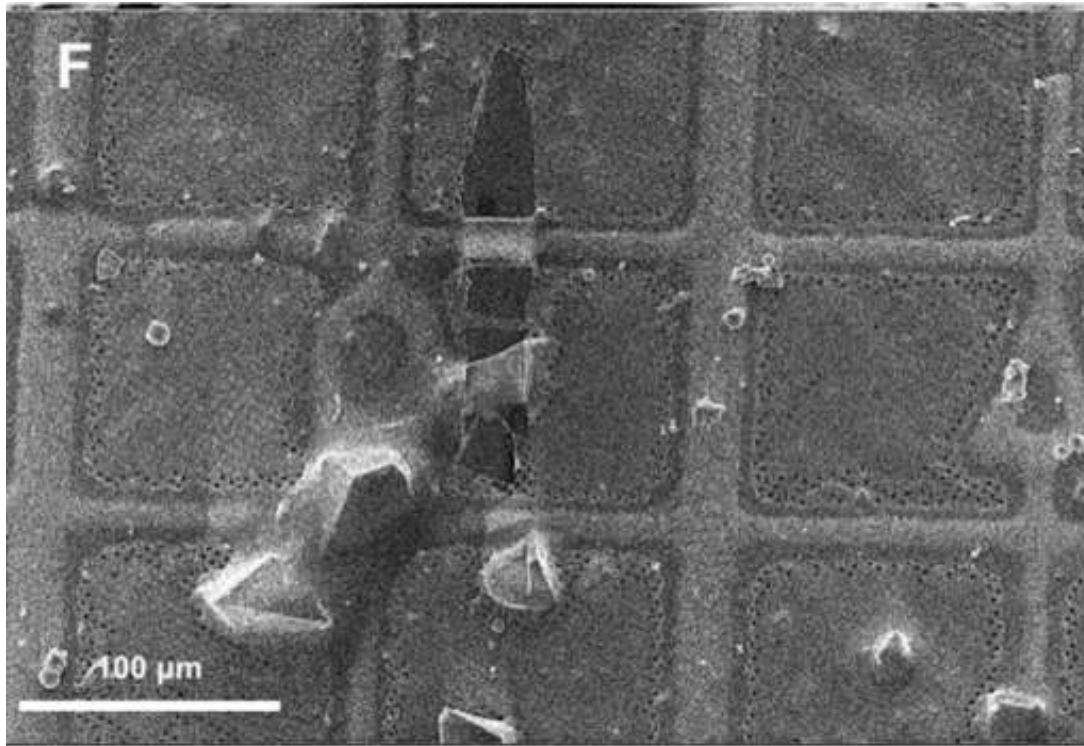


Ion beam view, before and after

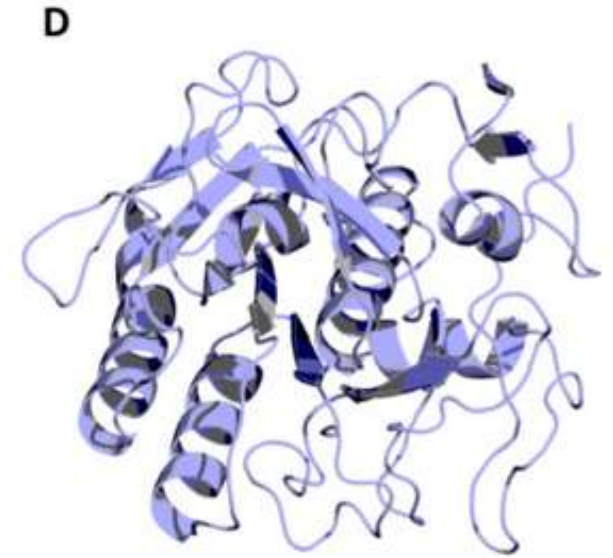
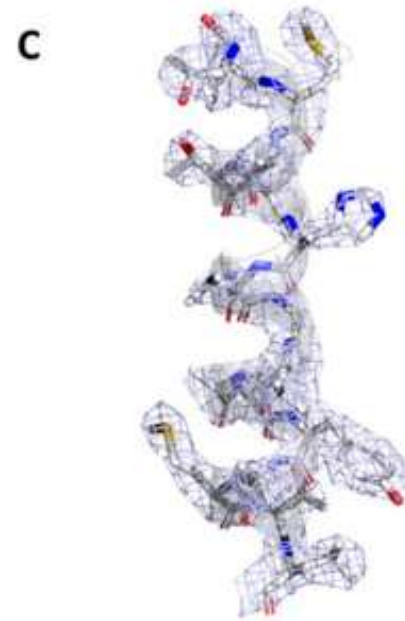
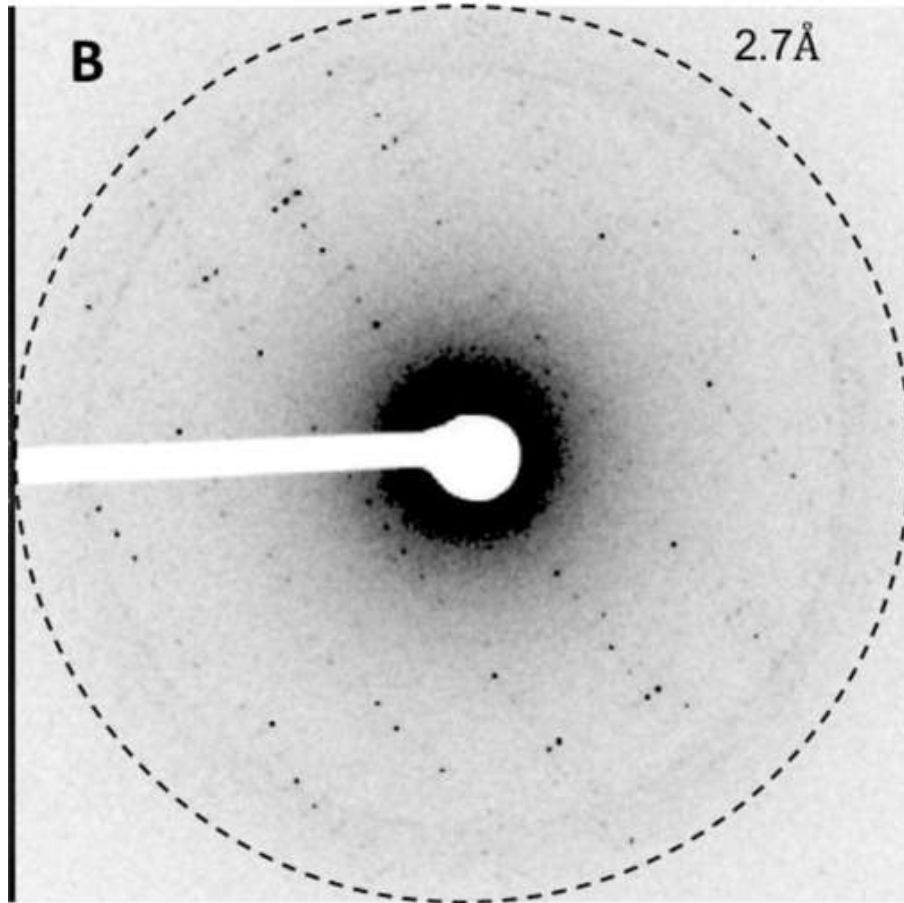


Thin to 300 nm

Ebeam: SEM and TEM



Proteinease K at 2.7 Å Resolution



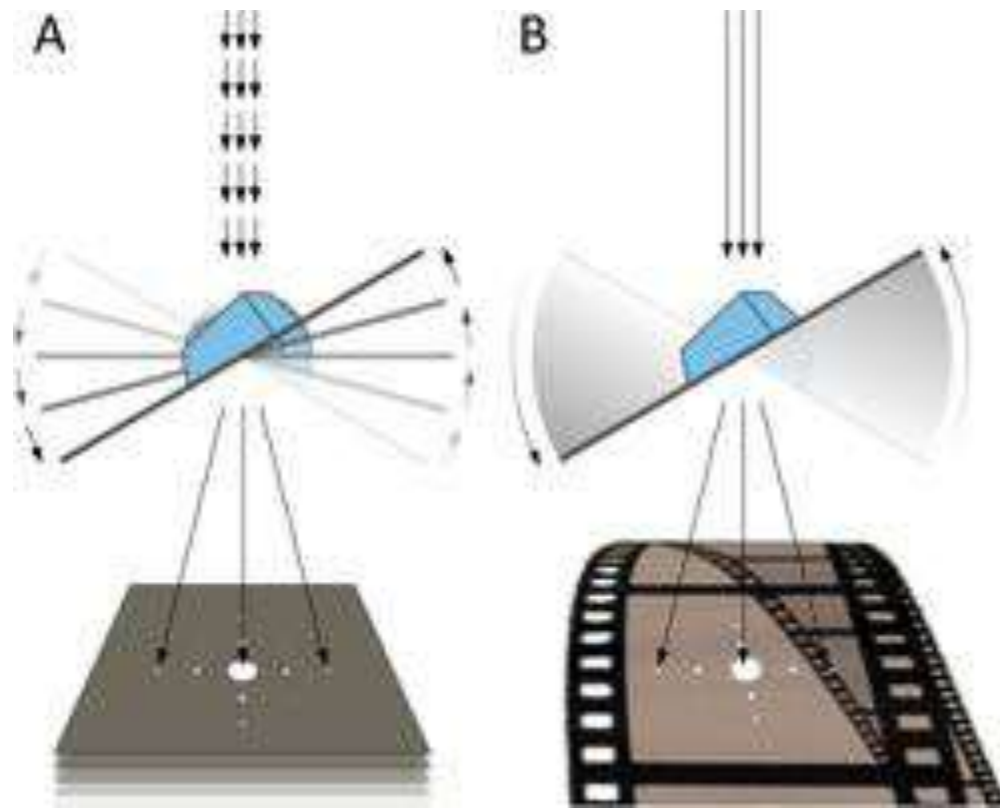
Data Collection: more specifics

- To date, most MicroED data was collected on a CMOS camera in “rolling shutter” mode
- Continuous readout of microscope parameters disabled
- In processing software, need to define
 - Beam Center
 - May not be center of image
 - May change due to microscope instabilities
 - Rotation rate of stage – angle and range of each frame
 - Need to record starting angle and direction (clockwise/counter-clockwise)
 - Virtual sample-detector distance
 - Calibrate from powder diffraction pattern of gold or graphite
- Conversion of movie to SMV (Super Marty View) format
 - Supported by x-ray software such as DIALS, MOSFLM, XDS

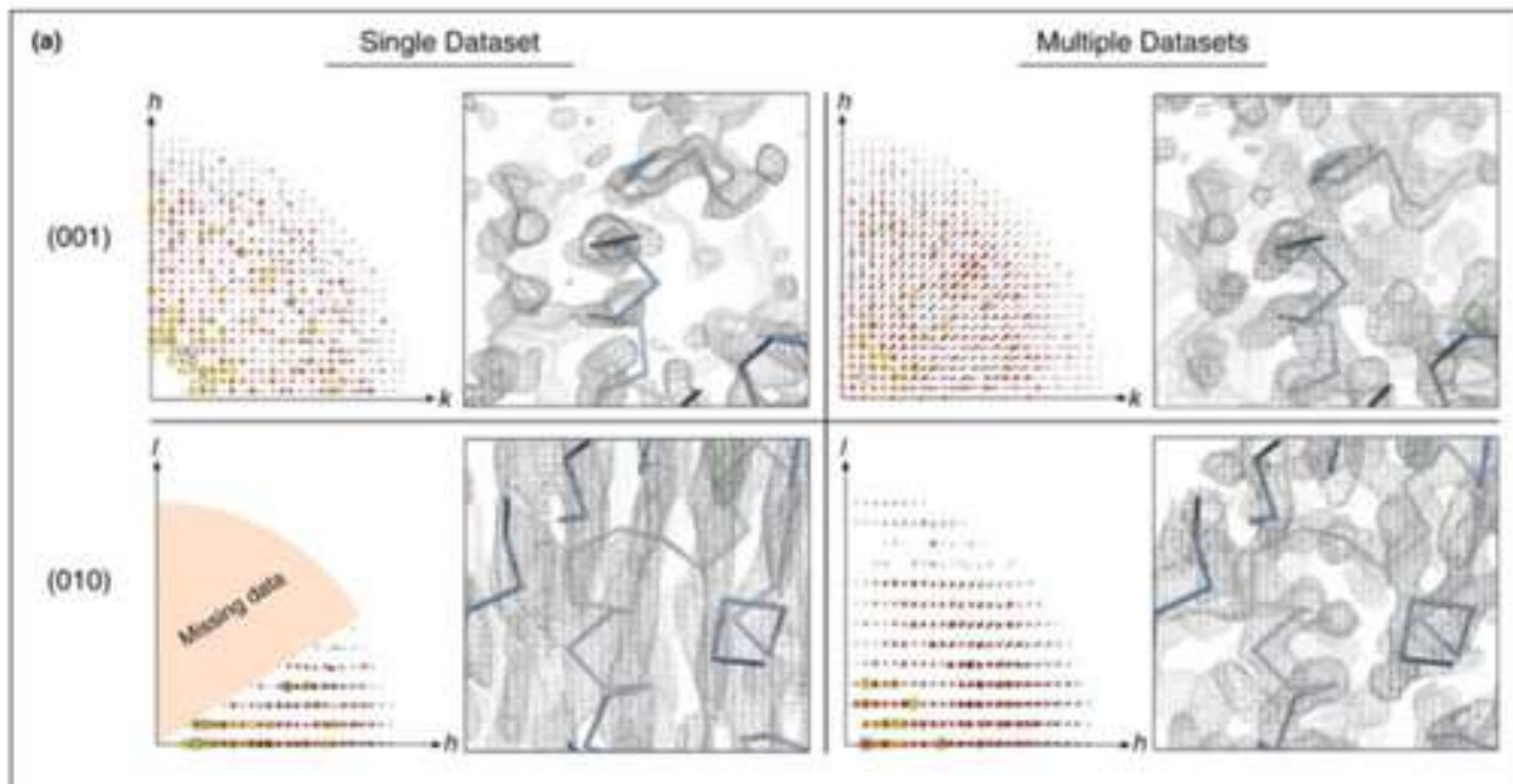
Collection

- Diffraction collection
 - 0.01-0.05 e/Å²/s
 - Exposure of 2-5s
 - If initial exposure shows good spots, collect continuous tilt series
 - Ideally -70° to +70° continuous collection
- Goniometer
 - Sample must be at eucentric height
 - Goniometer must be in good alignment so that sample does not slip out of field of view during tilt changes
- Sample
 - Must be thin: thickness varies with $1/\cos(a)$
- Camera
 - Needs to operate in continuous collection
 - Ceta or TVIPS F416: 'rolling shutter mode' (2048x2048, no microscope readout parameters)
 - Direct detector (Direct Electron DE series or Thermo Fisher Falcon III: Movie mode, high frame rate)
 - Dedicated diffraction camera: hybrid detector

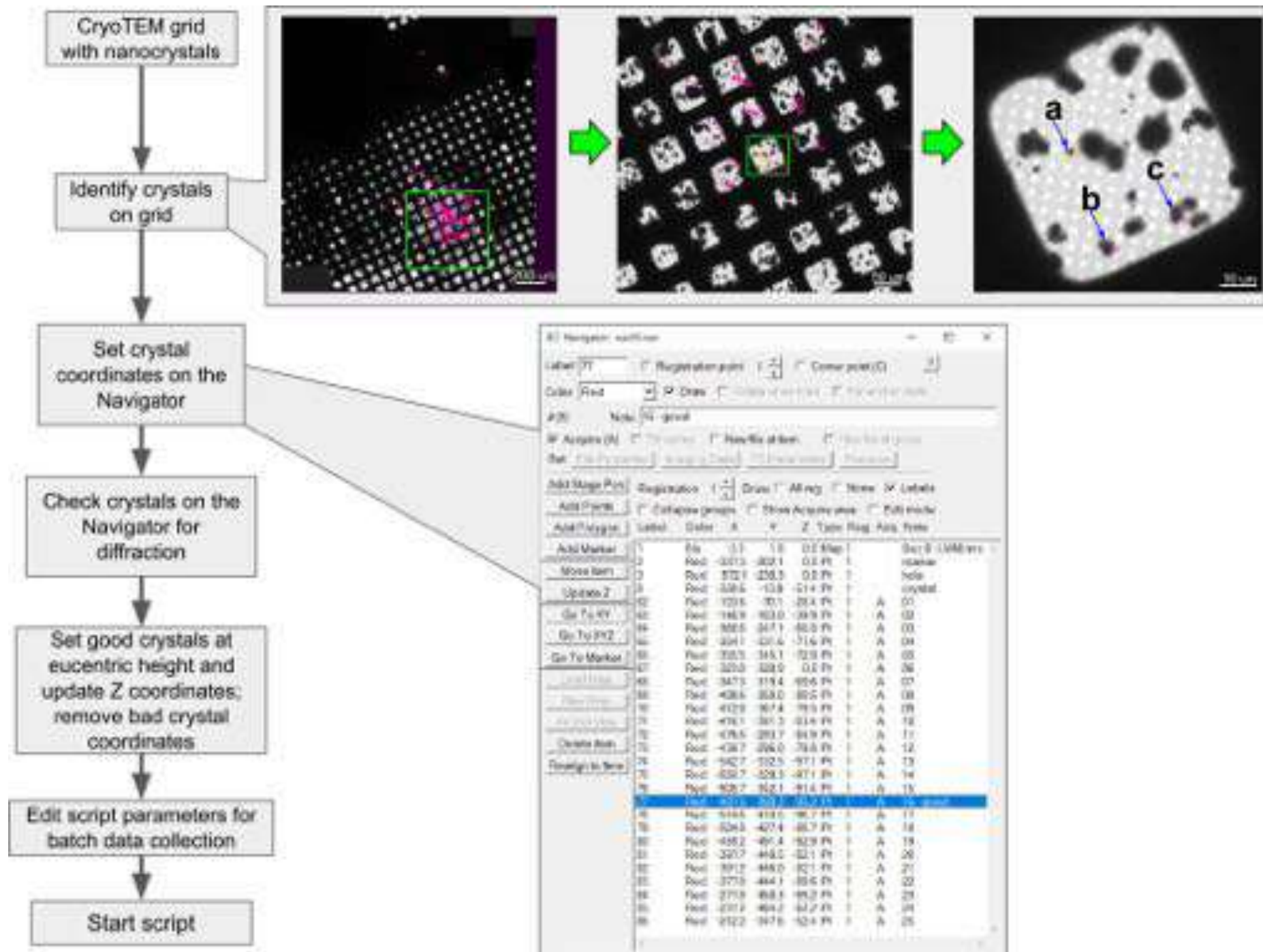
Modes of Collection



Missing Wedge (-70 to +70 degrees)



Automated Collection



Processing

- Movies need to be converted to a format readable by X-ray crystallography packages such as DIALS (Waterman et al 2013), MOSFLM (Leslie and Powell, 2007), and XDS (Kabsch, 2010)
- Super Marty View (SMV) can be read, conversion tools to SMV format exist
 - Interpretation of gain (ratio of variance to mean intensity in background regions)
 - Dead or hot pixels need to be flagged
 - Diffraction spots need to be in linear response region
- Most standard software needs a configuration file for the camera and microscope: camera length, wavelength, tilt axis

Crystal lattice determination (Indexing)

- More challenging than X-ray crystallography
- deBroglie wavelength $1/50$ that of X-ray
 - Ewald sphere less curved so spots fall within an almost planar wedge of reciprocal space
- Autoindexing relies on the 3D lattice to get spacing and orientation correct
- 5-10 images covering $\sim 20^\circ$ of continuous rotation are often enough to work
- Geometry of collection is less well defined
 - Calculate approximate orientation by multiplying frame time by rotation rate
 - Throw residual errors into the “mosaicity” of the crystal: error sink

Phasing

- For protein structures, phasing was done through molecular replacement
- Standard X-ray crystallography tools
- CNS, Phaser, phenix.refine, REFMAC all have electron scattering factors built in
- Ab initio phasing: works well for small molecules
 - Need diffraction to 1.4 Å or better

Extended Data Table: Same as for x-ray crystallography

Extended Data Table 1

Statistics of data collection and atomic refinement for NACore, its fragment SubNACore, and PreNAC.

| Segment | SubNACore AVVTGVTAV | NACore GAVVTGVTAVA | PreNAC GVVHGVTTVA |
|-----------------------------|------------------------|-----------------------|----------------------|
| Data collection | | | |
| Radiation source | Synchrotron | Electron | Electron |
| Space group | C2 | C2 | P21 |
| Cell dimensions | | | |
| a, b, c (Å) | 61.9, 4.80, 17.3 | 70.8, 4.82, 16.79 | 17.9, 4.7, 33.0 |
| α, β, γ (°) | 90, 104.1, 90 | 90, 105.7, 90 | 90, 94.3, 90 |
| Resolution (Å) | 1.85 (1.95–1.85) | 1.43 (1.60–1.43) | 1.41 (1.56–1.41) |
| Wavelength (Å) | 0.9791 | 0.0251 | 0.0251 |
| R_{merge} | 0.117 (0.282) | 0.173 (0.560) | 0.236 (0.535) |
| $R_{\text{r.i.m.}}$ | 0.135 (0.322) | 0.199 (0.647) | 0.264 (0.609) |
| $R_{\text{p.i.m.}}$ | 0.065 (0.154) | 0.093 (0.311) | 0.185 (0.305) |
| $I/\sigma I$ | 5.2 (2.7) | 5.5 (2.5) | 4.6 (1.8) |
| CC _{1/2} (%) | 99.5 (97.8) | 99.4 (92.3) | 96.7(74.0) |
| Completeness (%) | 97.9 (98.3) | 89.9 (82.6) | 86.9 (69.6) |
| Multiplicity | 4.1 (4.0) | 4.4 (4.3) | 3.7 (3.5) |
| Refinement | | | |
| Resolution (Å) | 1.85 (2.07–1.85) | 1.43 (1.60–1.43) | 1.41 (1.41–1.57) |
| No. reflections | 470 (125) | 1073 (245) | 1006 (239) |

*Highest resolution shell is shown in parenthesis.

Completeness

- Multi-crystal merging can increase completeness
 - But crystals need to land with different orientations on the grid
- One crystal often not enough: limited tilt range

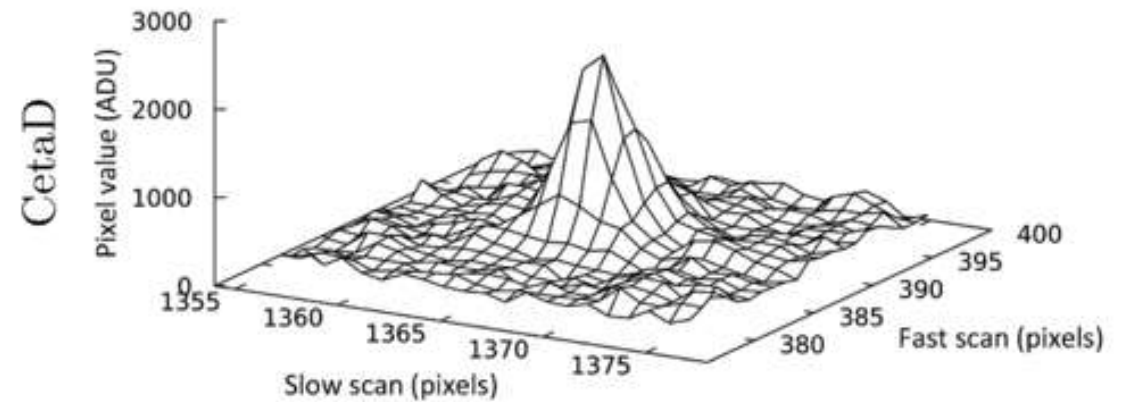
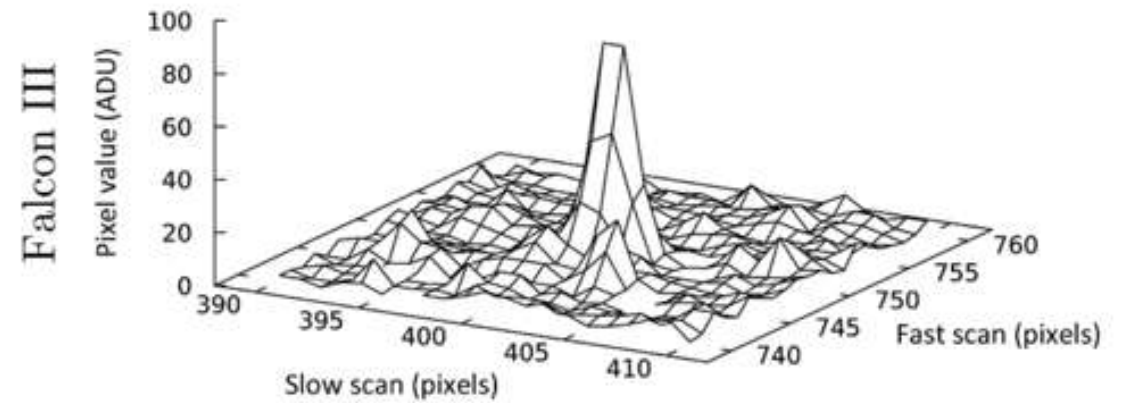
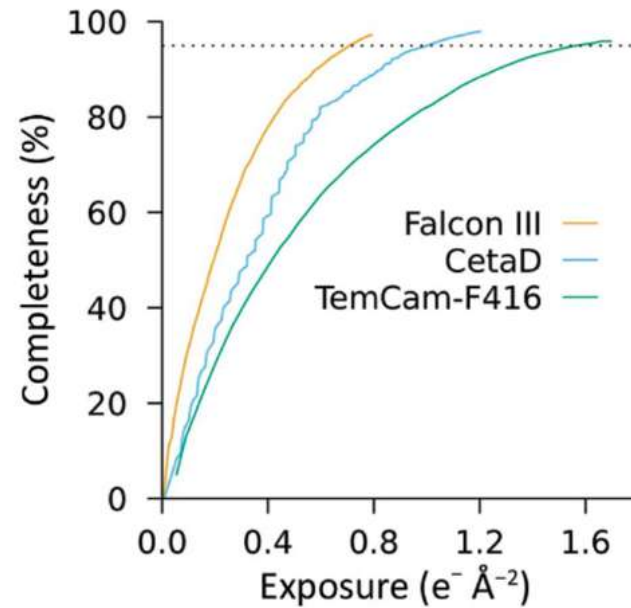
Detectors

- High dynamic range
- Fast readout low dead time (continuous rotation)
- Direct detectors: expensive, easily damaged
- TVIPS F416: 4kx4K CMOS detector with scintillation layer
 - Rolling shutter mode at 2kx2k available
- CetaD: 4Kx4K CMOS detector with thicker scintillation layer than standard Ceta camera
 - Rolling shutter mode available in software'
- Hybrid detectors: Medipix, Dectris,
 - High speed, high radiation hardness, high dynamic range
 - Large pixel size (75 μm), small number of pixels (up to 1k x 1k)

Falcon III

- Diffraction protection needs to be disabled by TFS (warranty)
- Rotate at $0.45^{\circ}/\text{sec}$, versus $0.30^{\circ}/\text{s}$ for CetaD
 - Exposure time FIII: 1s
 - CetaD: 1.55-3.06 s/frame
 - 129 frames on FIII; 71 frames CetaD
- 2.1Å resolution at FIII edge; 2.3-2.8 Å for CetaD
- Exposure rate $<0.01 \text{ e}/\text{\AA}^2/\text{s}$
- F416: 4-5s, exposure, $0.09^{\circ}/\text{sec}$ rotation, higher total exposure

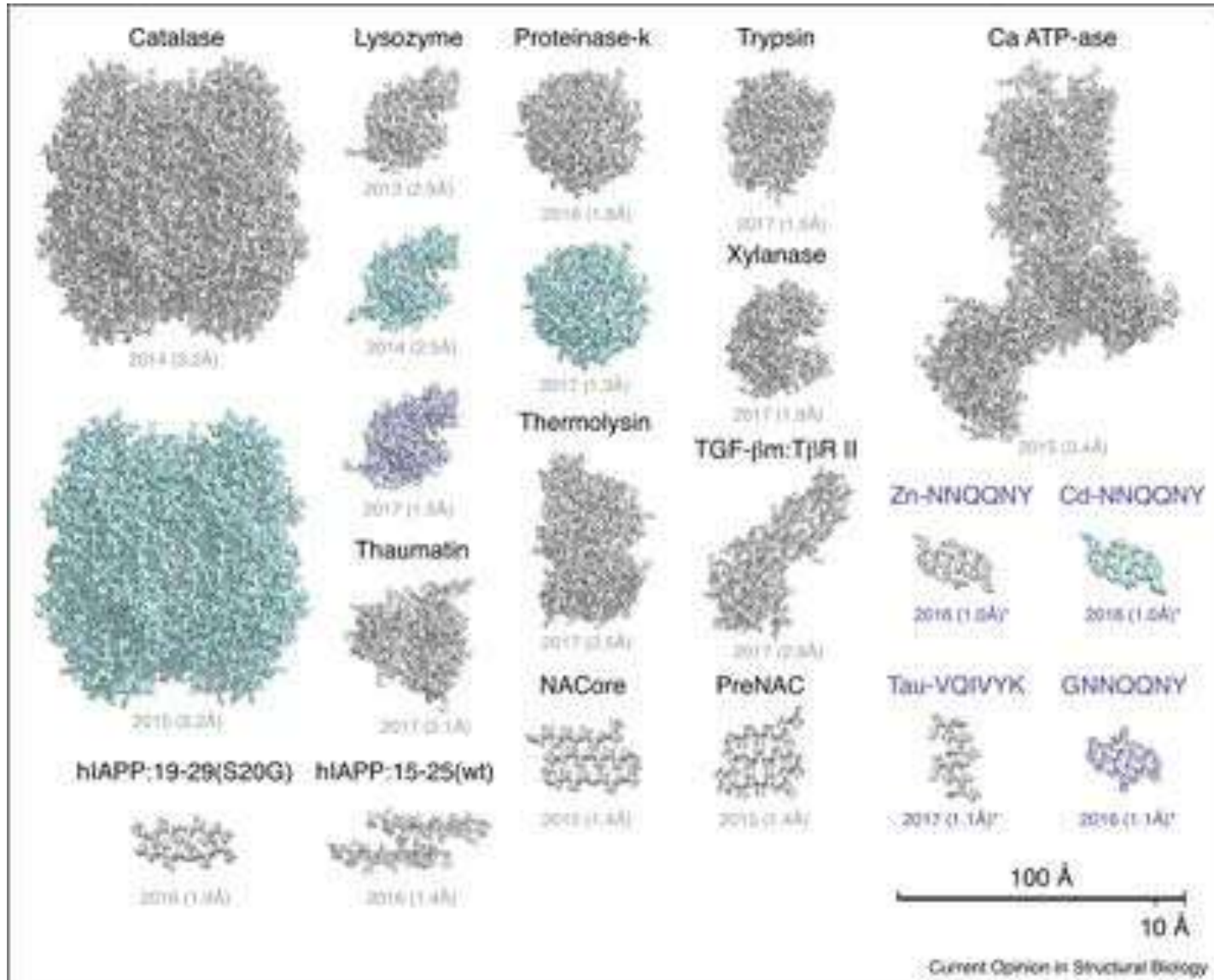
Falcon III for Detection



Hybrid Detectors

- EIGER (Tinti et al., 2018)
- Medipix (Nederlof et al., 2013)
- Timepix (van Genderen et al., 2016)
- Small size and large point spread function: dedicated diffraction cameras

Structures Solved by MicroED



Proteins all already solved by other means

Novel Structures

Solving a new R2lox protein structure by microcrystal electron diffraction

Hongyi Xu^{1,*†}, Hugo Lebrette^{2,†}, Max T. B. Clabbers^{1,†}, Jingjing Zhao¹, Julia J. Griesse^{2,3}, Xiaodong Zou^{1,*} and Martin Högbom^{2,*}

¹Department of Materials and Environmental Chemistry, Stockholm University, 10691 Stockholm, Sweden.

²Department of Biochemistry and Biophysics, Stockholm University, 10691 Stockholm, Sweden.

³Department of Cell and Molecular Biology, Uppsala University, 75124 Uppsala, Sweden.

✉*Corresponding author. Email: hongyi.xu@mmk.su.se (H.X.); hogbom@dbb.su.se (M.H.); xzou@mmk.su.se (X.Z.)

✉† These authors contributed equally to this work.

– Hide authors and affiliations

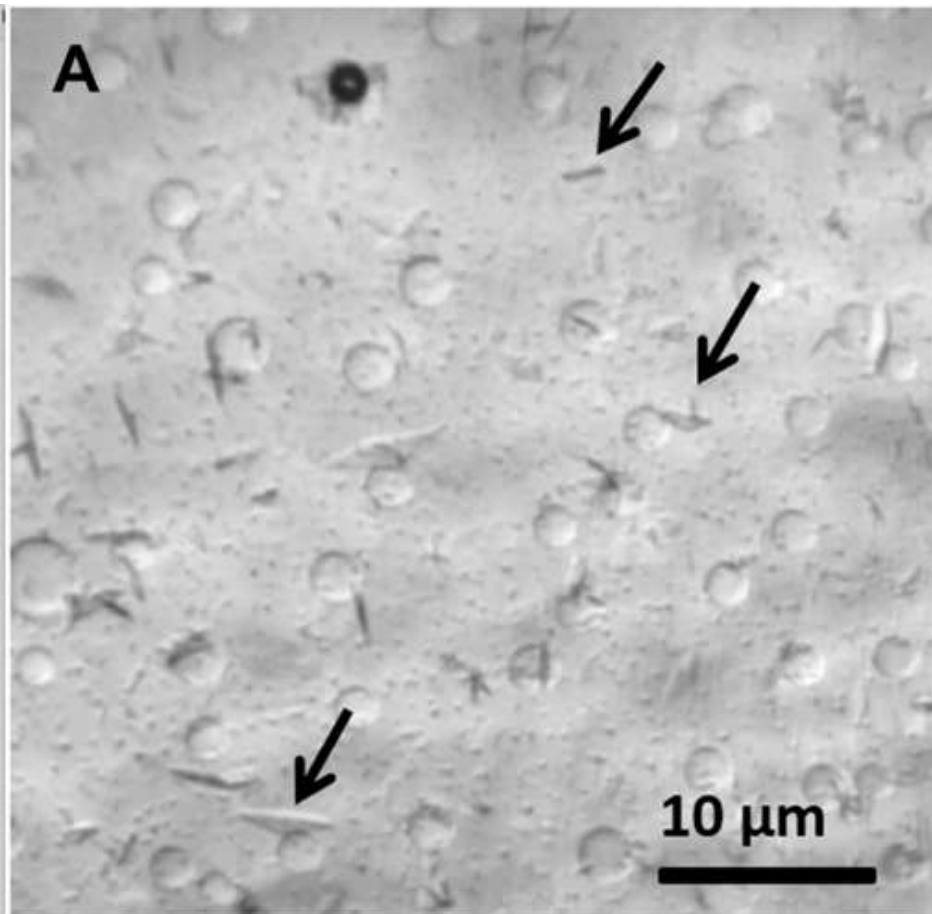
Science Advances 07 Aug 2019;
Vol. 5, no. 8, eaax4621
DOI: 10.1126/sciadv.aax4621

Continuous rotation method

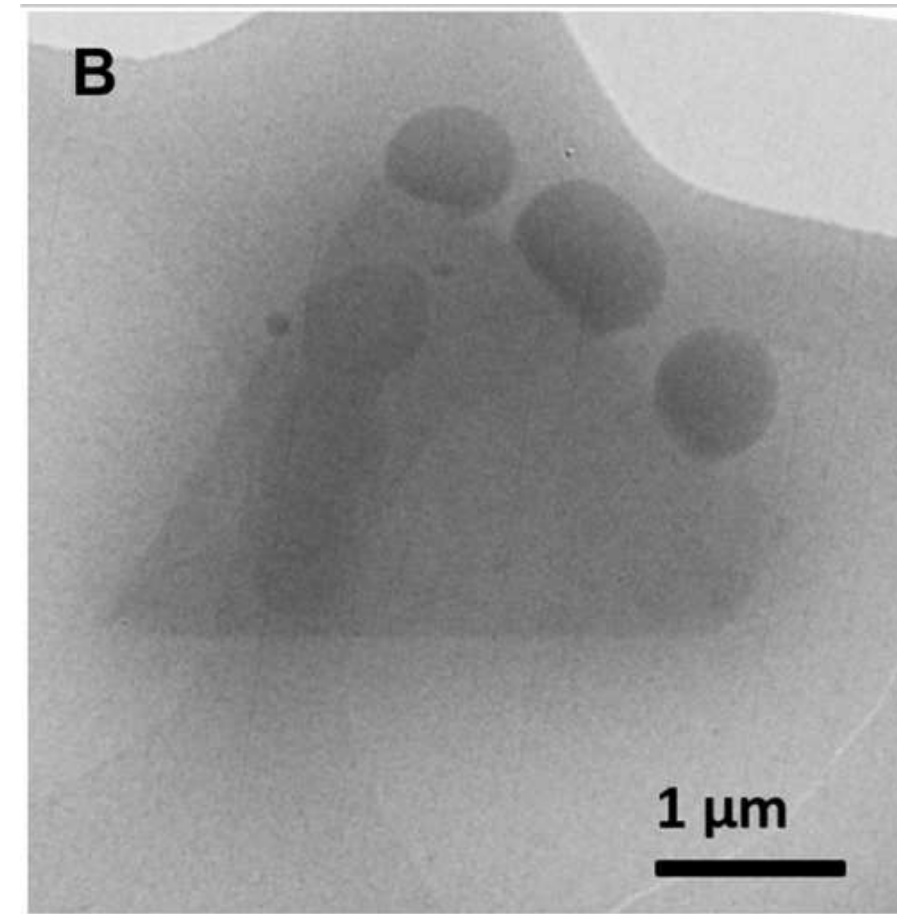
Conventional software: XDS , phasing with phaser (used protein with 35% sequence identity), refinement (phenix.refine)

Solving a new R2lox protein structure by microcrystal electron diffraction

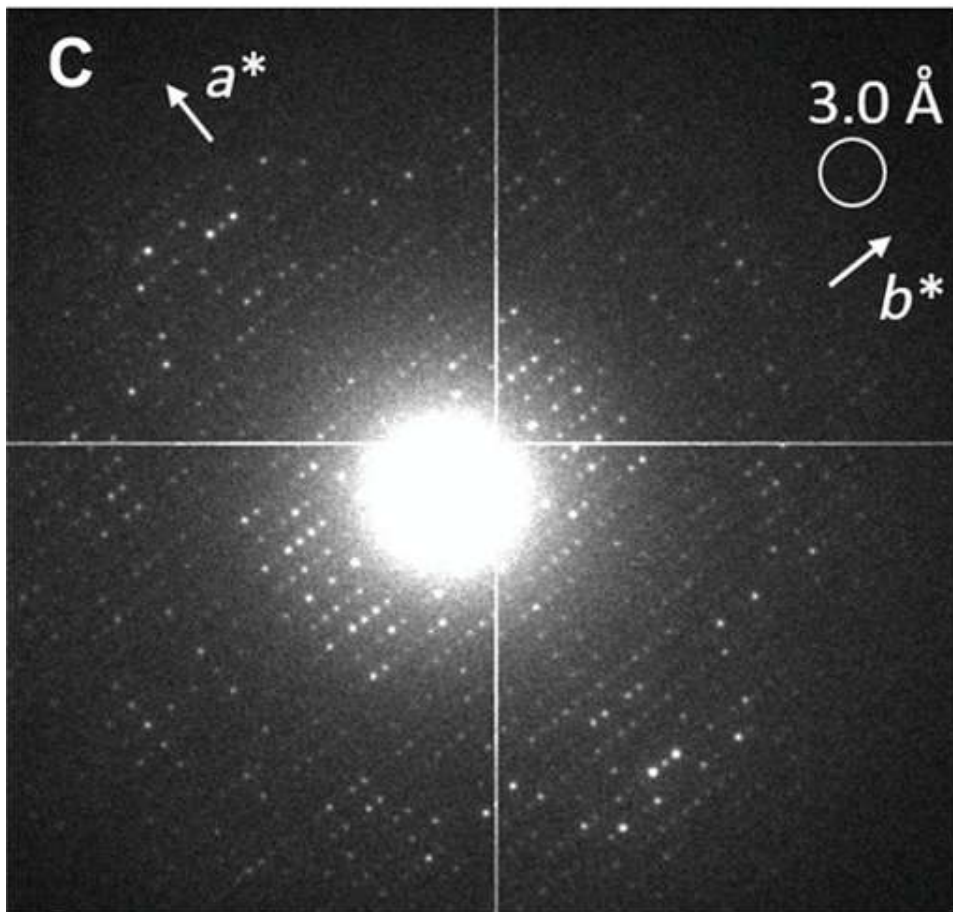
Hongyi Xu^{1,*†}, Hugo Lebrette^{2,†}, Max T. B. Clabbers^{1,†}, Jingjing Zhao¹, Julia J. Griese^{2,3}, Xiaodong Zou^{1,*} and Martin Högbom^{2,*}



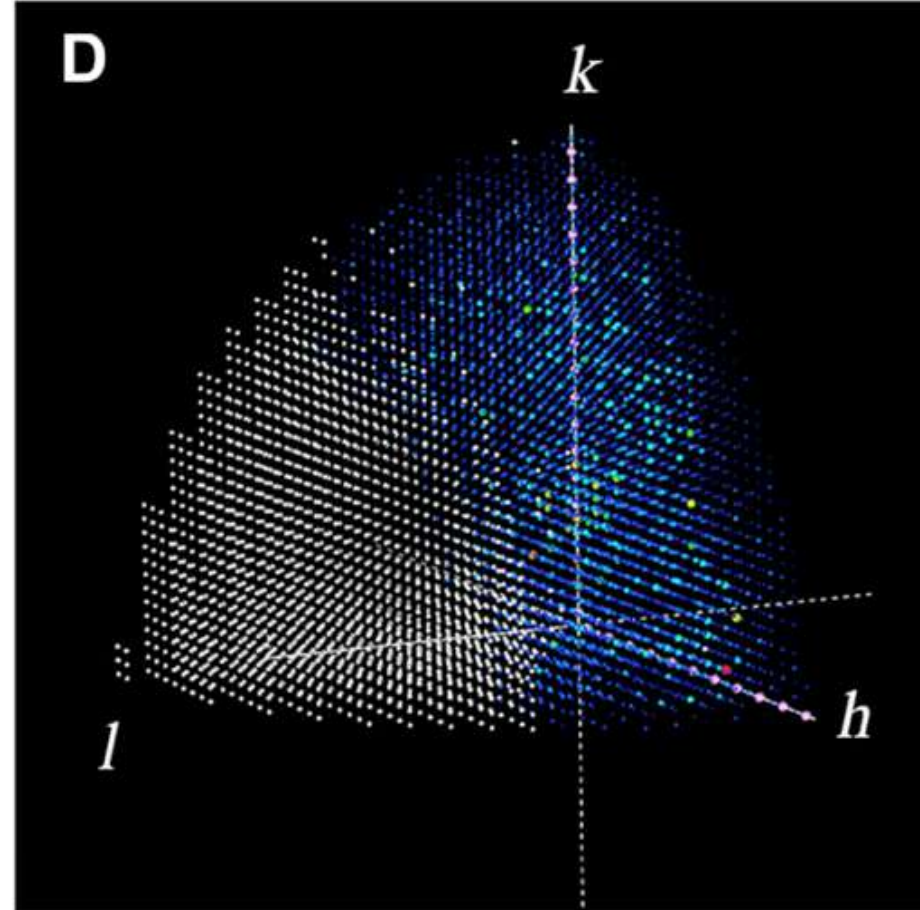
44% PEG 400; manual backside blot



Thickness < 0.5 μm
Plate-like crystals had preferred orientation

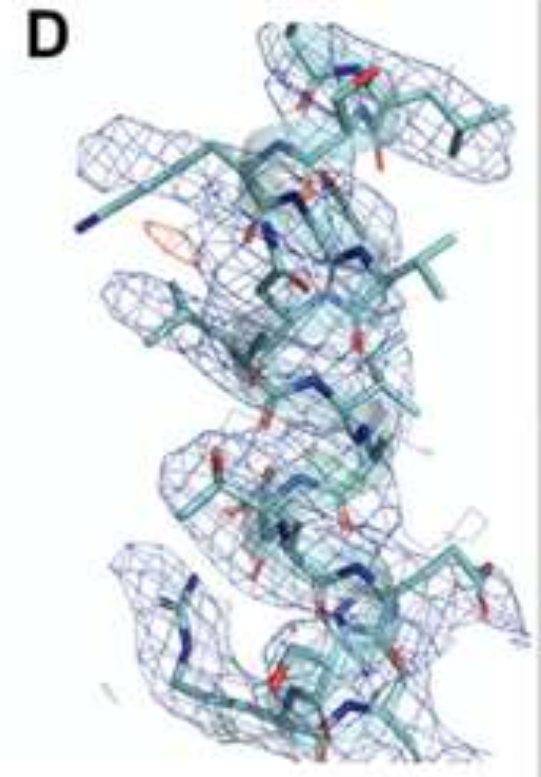
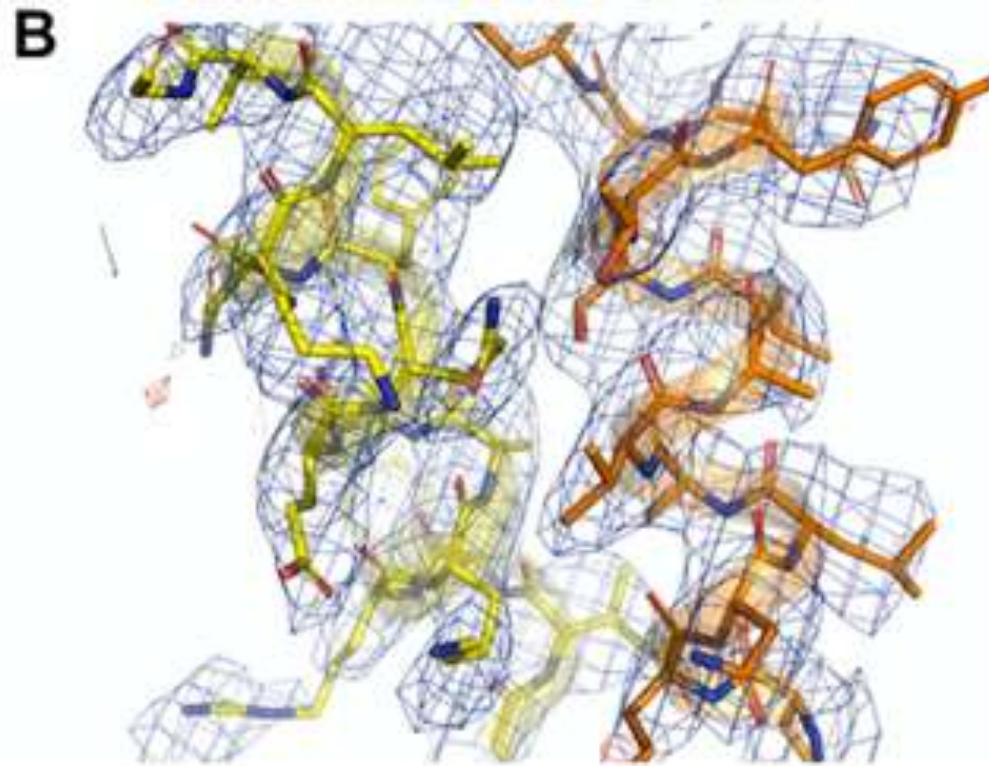
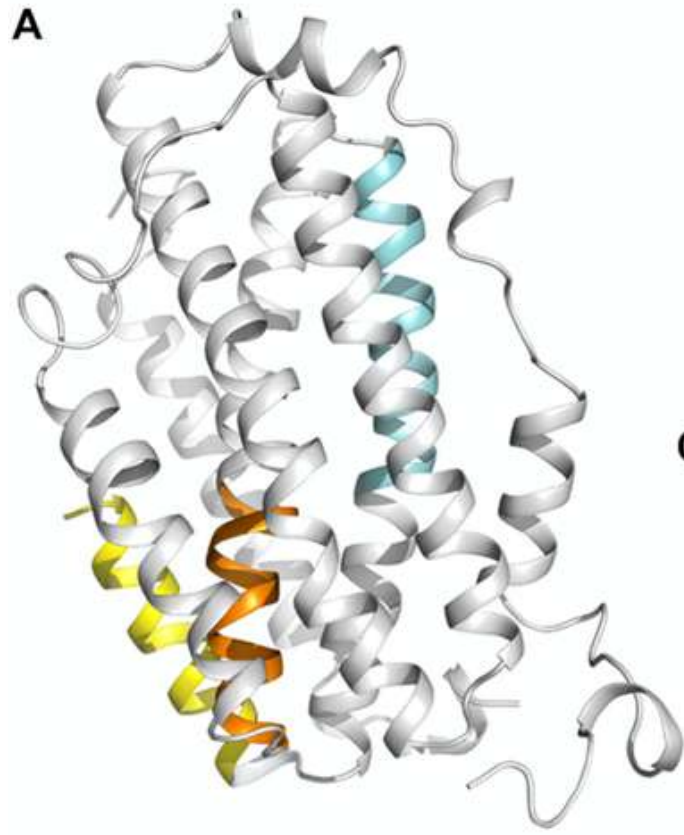


Completeness after merging 21 sets: 50.9% to 62.8%



Reconstructed reciprocal lattice showing limited data completeness with predominately missing reflections in the direction of c^* (fig. S1); missing observations are shown in white, observed reflections are in a rainbow color scheme, and systematic absences are shown in pink.

Maps



Scattering potential maps 2F0-Fc (blue), Fo-Fc (green,red)

Data Collection

- Microscope: JEOL JEM-2100, LaB₆ filament
- Crystal search: 50 μm C2 aperture (FOV 6 μm), side-entry Orius detector
- Collection: SA aperture 2 μm
- Detector: Timepix hybrid pixel detector
- 0.001198 \AA^{-1} / pixel (diffraction distance 1830 mm)

2018: Breakthrough for organic molecules

- Realized that quickly solving structures of small organic molecules (drugs and drug candidates) is highly desired
- Purified powders can be placed directly on an EM grid
 - Dry, not in solution
- Possible to image even at RT
- Possible to put multiple samples on one grid
- Each crystal collection is relatively fast
- Molecules small enough to solve by direct phasing methods

Small Molecules



Research Article

Cite This: ACS Cent. Sci. 2018, 4, 1587–1592

<http://pubs.acs.org/journal/acscii>

The CryoEM Method MicroED as a Powerful Tool for Small Molecule Structure Determination

Christopher G. Jones,^{†,‡} Michael W. Martynowycz,^{‡,§} Johan Hattne,[‡] Tyler J. Fulton,[§]
Brian M. Stoltz,^{*,§,●} Jose A. Rodriguez,^{*,†,||} Hosea M. Nelson,^{*,†} and Tamir Gonen^{*,‡}

[†]Department of Chemistry and Biochemistry, [‡]Howard Hughes Medical Institute, David Geffen School of Medicine, Departments of Biological Chemistry and Physiology, and [§]UCLA-DOE Institute, University of California, Los Angeles, California 90095, United States

[●]The Warren and Katharine Schlinger Laboratory of Chemistry and Chemical Engineering, California Institute of Technology, Pasadena, California 91125, United States

 Communication Information

Small Molecules

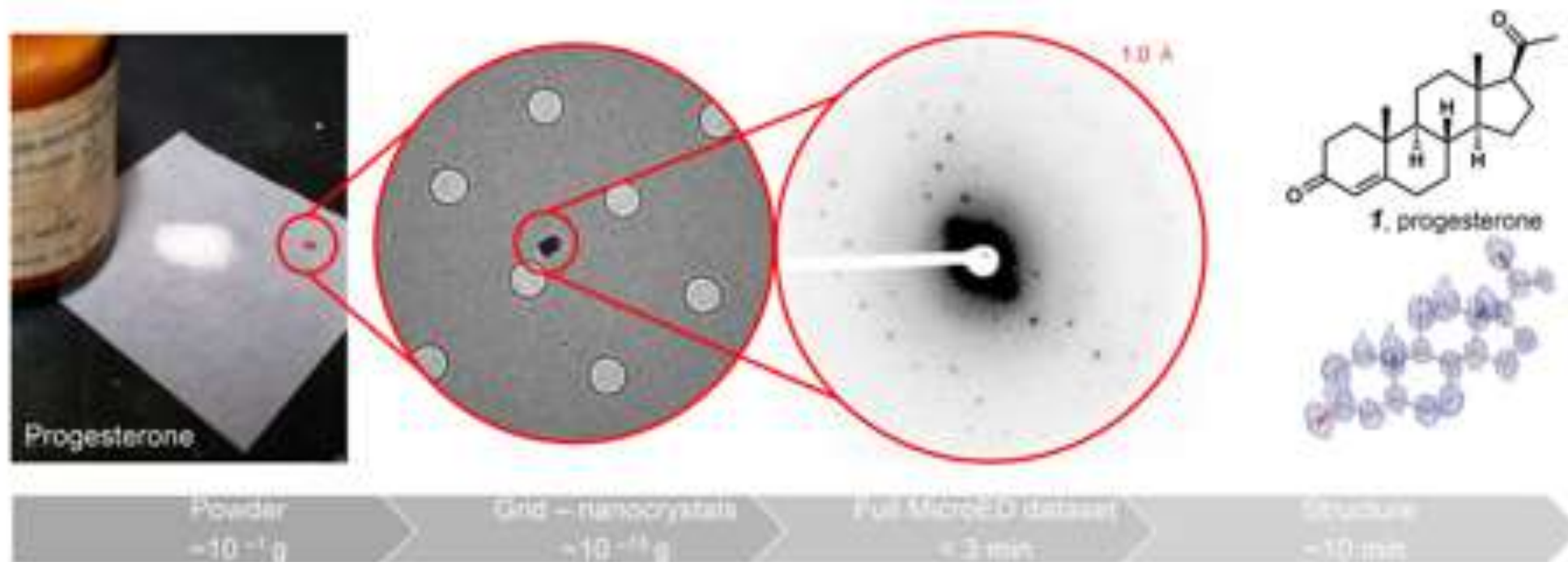


Figure 1. Process of applying MicroED to small molecule structural analysis. Here commercial progesterone (**1**) was analyzed, and an atomic resolution structure was determined at 1 Å resolution. Grid holes are 1 μm in diameter.

Small Molecules

A



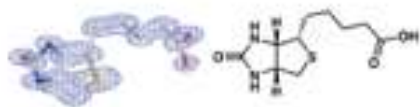
acetaminophen, 2



ibuprofen, 3



carbamazepine, 4



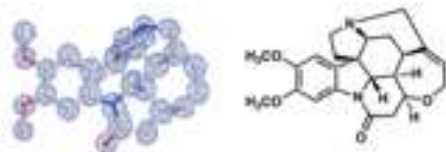
biotin, 6



ethisterone, 7



cinchonine, 8



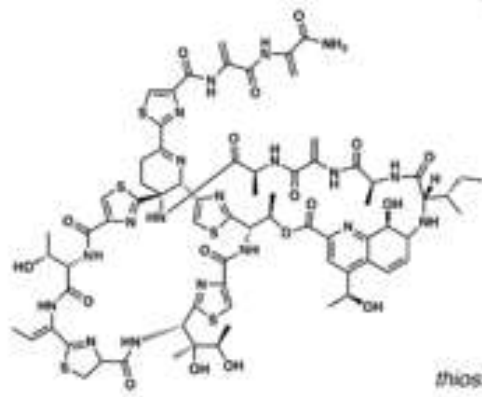
brucine, 9



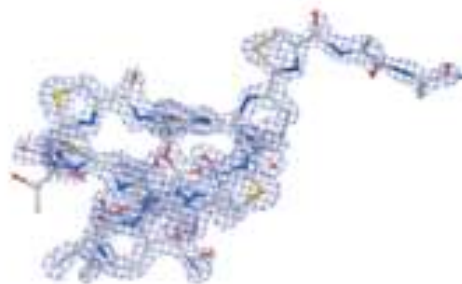
synthetic (+)-
limaspermidine, 10



synthetic oxindole,
HKL-1-029, 11



thiostrepton, 5



Small Molecules: Flask to Structure

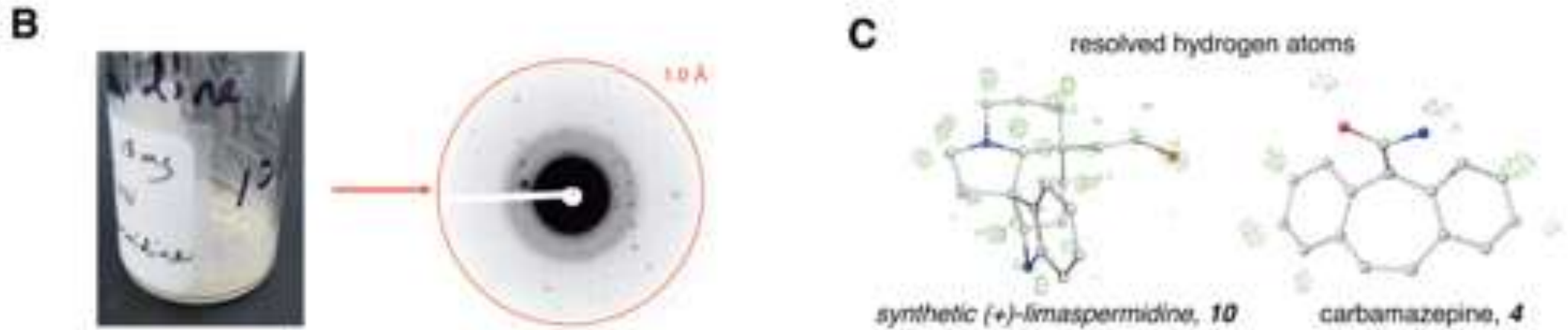


Figure 2. Different types of small molecules solved by MicroED. (A) Several pharmaceuticals, vitamins, commercial natural products, and synthetic samples resolved through MicroED. (B) Example of an amorphous film utilized in this study leading to 1 Å resolution data. (C) Protons could be observed for several compounds through MicroED. Green density are $F_o - F_c$ maps showing positive density belonging to hydrogen atoms of the molecule.

What do you need for MicroED?

Detectors



- CCD

- Older technology
- Slow readout: no continuous collection

- CMOS with scintillation layer

- Continuous collection possible in rolling shutter mode or movie mode
- TVIPS F416, Thermo Fisher Ceta, CetaD
- Commonly installed on mid-high end microscopes



- Direct Detector

- Continuous collection in movie mode
- Dangerous: easily damaged

Detectors

- Hybrid Detector
 - Dectris, Timepix
 - Radiation hardened, high dynamic range
 - Large pixel size (e.g. 75 x 75 μm for Dectris Eiger2)
 - Small: 512x512, 1k x 1k – currently not suitable for imaging applications

Microscopes

- Voltage:
 - 200 keV, 300 keV
 - Enough for thickness up to ~400 nm
- Emission
 - FEG desirable but not essential
- Goniometer
 - Must be very well aligned to allow for continuous rotation of constant viewing area
- Stable cryo holder
 - If doing proteins
 - Powder can be done at RT
- Custom SA apertures
 - Typical: 800 μm , 200 μm , 40 μm , 10 μm
 - Better: 200 μm , 150 μm , 70 μm , 40 μm
- Slim beamstop to not lose low-resolution data
 - Important for protein crystals, small molecules not as necessary

Sample method: Proteinase K

- Proteinase K from Engyodontium album(Sigma–Aldrich, StLouis, Missouri, USA)
- Dissolve in 50 mM Tris-HCl pH 8 (50 mg/ml)
- Mix with equal volume of 1.25 M ammonium sulfate
- Dispense into 24 well plates, crystals appear in 1h in sitting drops
- Sitting drops diluted to 25 μ l with well solution, pipette 2 μ l onto carbon side of Quantifoil R 2/2 Cu300 grid
- Blot back side 5s, 4 °C, 100% humidity

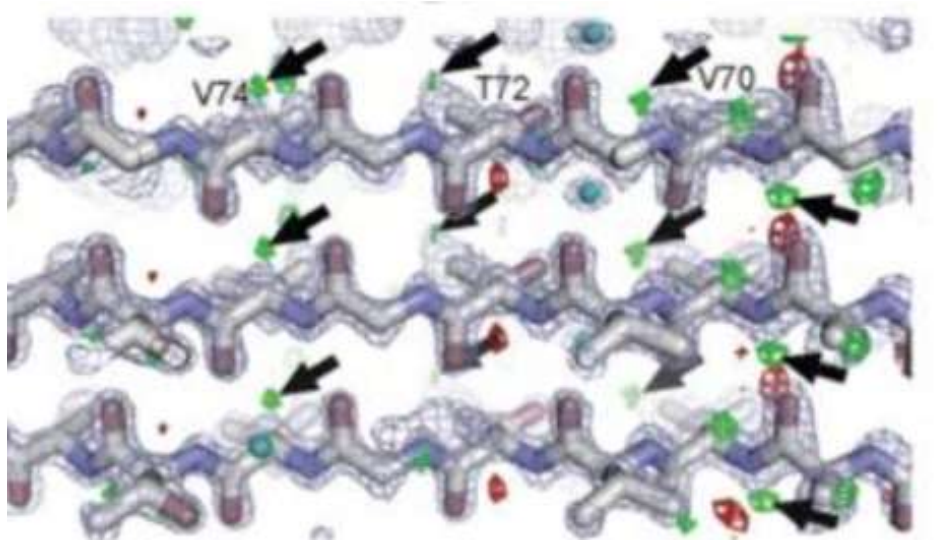
Future Directions

- Other methods for phasing besides molecular replacement
- Improvement of detectors: larger hybrid detectors
- Improvements in collection software
- FIB milling possibly becoming more popular for thicker crystals

Summary

- Advantages
 - Mid-level equipment (200 keV, FEG, CMOS detector with movie mode)
 - Alignment probably less difficult than for imaging mode
 - Highest resolution yet achieved by cryo-EM technique
 - Processing software (X-ray) mature and well understood by a large community
 - Sample prep for small molecules is relatively simple
- Disadvantages
 - Crystals must be small (400 nm max thickness) and randomly oriented
 - FIB if necessary
 - Sample prep and screening for proteins is difficult
 - High quality stage essential, continuous tilting collection needed
 - Phasing problem: molecular replacement needed for most protein structures

Questions



References

1. de la Cruz, M.J., et al., *Atomic-resolution structures from fragmented protein crystals with the cryoEM method MicroED*. Nat Methods, 2017. **14**(4): p. 399-402.
2. de la Cruz, M.J., et al., *MicroED data collection with SerialEM*. Ultramicroscopy, 2019. **201**: p. 77-80.
3. Hattne, J., et al., *MicroED with the Falcon III direct electron detector*. IUCr, 2019. **6**(Pt 5): p. 921-926.
4. Hattne, J., et al., *MicroED data collection and processing*. Acta Crystallogr A Found Adv, 2015. **71**(Pt 4): p. 353-60.
5. Hattne, J., et al., *Modeling truncated pixel values of faint reflections in MicroED images*. J Appl Crystallogr, 2016. **49**(Pt 3): p. 1029-1034.
6. Hattne, J., et al., *Analysis of Global and Site-Specific Radiation Damage in Cryo-EM*. Structure, 2018. **26**(5): p. 759-766 e4.
7. Jones, C.G., et al., *The CryoEM Method MicroED as a Powerful Tool for Small Molecule Structure Determination*. ACS Cent Sci, 2018. **4**(11): p. 1587-1592.
8. Krotee, P., et al., *Atomic structures of fibrillar segments of hIAPP suggest tightly mated beta-sheets are important for cytotoxicity*. Elife, 2017. **6**.
9. Liu, S., et al., *Atomic resolution structure determination by the cryo-EM method MicroED*. Protein Sci, 2017. **26**(1): p. 8-15.
10. Martynowycz, M.W., et al., *Qualitative Analyses of Polishing and Precoating FIB Milled Crystals for MicroED*. Structure, 2019. **27**(10): p. 1594-1600 e2.
11. Martynowycz, M.W., et al., *Collection of Continuous Rotation MicroED Data from Ion Beam-Milled Crystals of Any Size*. Structure, 2019. **27**(3): p. 545-548 e2.
12. Nannenga, B.L. and T. Gonen, *The cryo-EM method microcrystal electron diffraction (MicroED)*. Nat Methods, 2019. **16**(5): p. 369-379.
13. Nannenga, B.L. and T. Gonen, *MicroED: a versatile cryoEM method for structure determination*. Emerg Top Life Sci, 2018. **2**(1): p. 1-8.
14. Nannenga, B.L. and T. Gonen, *MicroED opens a new era for biological structure determination*. Curr Opin Struct Biol, 2016. **40**: p. 128-135.
15. Nannenga, B.L. and T. Gonen, *Protein structure determination by MicroED*. Curr Opin Struct Biol, 2014. **27**: p. 24-31.
16. Nannenga, B.L., et al., *Structure of catalase determined by MicroED*. Elife, 2014. **3**: p. e03600.
17. Nannenga, B.L., et al., *High-resolution structure determination by continuous-rotation data collection in MicroED*. Nat Methods, 2014. **11**(9): p. 927-930.
18. Purdy, M.D., et al., *MicroED structures of HIV-1 Gag CTD-SP1 reveal binding interactions with the maturation inhibitor bevirimat*. Proc Natl Acad Sci U S A, 2018. **115**(52): p. 13258-13263.
19. Sawaya, M.R., et al., *Ab initio structure determination from prion nanocrystals at atomic resolution by MicroED*. Proc Natl Acad Sci U S A, 2016. **113**(40): p. 11232-11236.
20. Shi, D., et al., *The collection of MicroED data for macromolecular crystallography*. Nat Protoc, 2016. **11**(5): p. 895-904.
21. Shi, D., et al., *Three-dimensional electron crystallography of protein microcrystals*. Elife, 2013. **2**: p. e01345.
22. Xu, H., et al., *Solving a new R2lox protein structure by microcrystal electron diffraction*. Sci Adv, 2019. **5**(8): p. eaax4621.
23. Gonen, T., *The collection of high-resolution electron diffraction data*. Methods Mol Biol, 2013. **955**: p. 153-69.
24. Wisedchaisri, G., S.L. Reichow, and T. Gonen, *Advances in structural and functional analysis of membrane proteins by electron crystallography*. Structure, 2011. **19**(10): p. 1381-93.